

**SYNTHESIS AND CHARACTERIZATION OF EXTENDED GRAPHITE  
SHEET/ZnO NANOCOMPOSITE ELECTROCHEMICAL SENSOR FOR  
THE DETECTION OF PARA-NITROPHENOL**

**MSc THESIS**

**MULU TAJEBE MEKONEN**

**JUNE 2018**

**HARAMAYA UNIVERSITY, HARAMAYA**

**Synthesis and Characterization of Extended Graphite Sheet/ZnO Nanocomposite Electrochemical Sensor for the Detection of para-Nitrophenol**

**A Thesis Submitted to the Department of Chemistry,  
Postgraduate Program Directorate  
HARAMAYA UNIVERSITY**

**In partial Fulfillment of the Requirements for the Degree of  
MASTER OF SCIENCE IN CHEMISTRY**

**Mulu Tajebe Mekonen**

**JUNE 2018**

**Haramaya University, Haramaya**



## STATEMENT OF THE AUTHOR

By my signature below, I state and affirm that this Thesis is my own work. I have followed all ethical and technical principles in the preparation, data collection, data analysis and compilation of this Thesis. Any Scholarship matter that is included in the Thesis has been given recognition through citation.

This Thesis is submitted in partial fulfillment of the requirements for MSc degree at the Haramaya University and is made available to borrowers under the rules of the Library. I solemnly declare that this Research Thesis has not been submitted to any other institution anywhere for the award of any academic degree, diploma or certificate.

Brief quotations from this Research Thesis may be made without special permission provided that accurate and complete acknowledgment of the source is made. Requests for permission for extended quotation from or reproduction of this Thesis in whole or part may be granted by the Head of the School or Department when in this or her judgment the proposed use of material is in the interest of scholarship. In all other instances, however, permission must be obtained from the author of the Thesis.

Name: MuluTajebe

Signature \_\_\_\_\_

Date: \_\_\_\_\_

Department: Chemistry

## **BIOGRAPHICAL SKETCH OF THE AUTHOR**

The author was born on June 12, 1986 in AsgedeTsimbla woreda, south west Zone, Tigray region. He first started his primary education in Endabaguna Elementary and Secondary school in 1997. He attended his preparatory school at Shire Endaselsie Preparatory School. After completing preparatory school, he then joined Axum University, Department of Chemistry in 2008 and graduated with BEd degree in Chemistry in 2010. Soon after graduation, the author was employed by MOE in 2011 to work under the Oromia Education Bureau, East Showa Zone, Boset Woreda as a teacher. After three years service, he joined Haramaya University, College of Natural and Computational Sciences, Department of Chemistry in 2013 to pursue his postgraduate studies in Chemistry under the summer postgraduate program.

## **ACKNOWLEDGEMENTS**

I would like to thank my advisor Dr. AbebawAdgo for his valuable scientific comments and guidance from the beginning of my work based on continuous, excellent and timely advices, close follow up supervision throughout all my work and reading the manuscript. In parallel to this, my special heart full thanks also goes to my co-advisor Dr. EndaleTeju for his close fatherly approach, guidance, coordination, valuable comments, suggestions and encouragement.

I am deeply grateful to the Ministry of Education for the financial support to complete my thesis and the Department of Chemistry, Haramaya University for unreserved help and encouraging me by providing necessary materials.

I gratefully acknowledge Addis Ababa University for characterizing the sample using FTIR and XRD analysis and Drie leather industry for sample preparations that help me in sample preparation.

Last but not the least I wish to thank my family and friends for their moral support, consistent encouragement and valuable advices.

## ACRONYMS AND ABBREVIATIONS

CMEs	Chemically Modified Electrodes
CPE	Carbon Paste Electrode
CV	Cyclic Voltametry
DPV	Differential Pulse Voltametry
E	Potential
EGS	Extended Graphite Sheet
EIS	Electrochemical Impedance Spectroscopy
EPa	Anodic Peak Potential
EPc	Cathodic Peak Potential
GCE	Glass Carbon Electrode
GO	Graphite Oxide
LOD	Limit of Detection
NP	Nitrophenol
NPs	Nanoparticles
PBS	Phosphate Buffer Solutions
P-NP	Para-Nitrophenol
rGO	Reduced Graphene Oxide
USEPA	United State Environmental Protection Agency

## TABLE OF CONTENTS

<b>STATEMENT OF THE AUTHOR</b>	<b>iii</b>
<b>BIOGRAPHICAL SKETCH OF THE AUTHOR</b>	<b>iv</b>
<b>ACKNOWLEDGEMENTS</b>	<b>v</b>
<b>ACRONYMS AND ABBREVIATIONS</b>	<b>vi</b>
<b>LIST OF TABLES</b>	<b>x</b>
<b>LIST OF FIGURES</b>	<b>xi</b>
<b>LIST OF TABLES IN APPENDIX</b>	<b>xiii</b>
<b>ABSTRACT</b>	<b>xiv</b>
<b>1. INTRODUCTION</b>	<b>1</b>
<b>2. LITERATURE REVIEW</b>	<b>6</b>
<b>2.1. Phenolic Compounds</b>	<b>6</b>
<b>2.2. Environmental Pollution by Phenolic Compounds</b>	<b>8</b>
<b>2.3. Method of Determination of Phenolic Compounds</b>	<b>10</b>
2.3.1. Spectroscopic and Chromatographic Determination	10
2.3.2. Electrochemical Methods of Determination of Phenol Compounds	11
<b>2.4. Chemical Sensors</b>	<b>13</b>
<b>2.5. Electrochemical Sensor</b>	<b>13</b>
<b>2.6. Working Principle for Detecting of Para-Nitrophenol</b>	<b>14</b>
2.6.1. Chemically Modified Electrodes (CMEs)	14
<b>2.7. Nanomaterials for Modified Electrodes</b>	<b>15</b>
2.7.1. Nanoparticles	15
2.7.2. Bimetallic Nanoparticles	16
2.7. 3. Metal Oxides Nanoparticles	16
2.7.4. Carbon Nanomaterials	17
2.7.5. Graphene Oxide (GO)	18
2.7.6. Reduced Graphite Oxide	19
2.7.7. Carbon Nanotubes	20
<b>2.8. Methods of Synthesis of Nanoparticles</b>	<b>21</b>
2.8.1. Electrochemical Reduction	21
2.8.2. Sol-Gel Reaction Method	21

continues...

2.8.3. Chemical Precipitation Method	22
2.8.4. Hydrothermal Method	22
2.8.5. Impregnation Method	22
2.8.6. Chemical Reduction Method	23
<b>2.9. Electrochemical Techniques</b>	<b>23</b>
2.9.1. Cyclic Voltammetry	23
2.9.2. Differential Pulse Voltammetry	26
<b>3. MATERIALS AND METHODS</b>	<b>28</b>
<b>3.1. Experimental Site</b>	<b>28</b>
<b>3.2. Instruments and Apparatus</b>	<b>28</b>
<b>3.3. Reagents and Chemicals</b>	<b>29</b>
<b>3.4. Experimental Procedures for the Synthesis of Nanocomposites</b>	<b>29</b>
3.4.1. Synthesis of Extended Graphite Sheet	29
3.4.2. Synthesis of ZnO Nanoparticle	29
3.4.3. Synthesis of Extended Graphite Sheet/ZnO Nanocomposite	30
3.4.4. Preparation of Buffer Solution	30
<b>3.5. Structural Characterization of the As-Synthesized NPs</b>	<b>31</b>
3.5.1. X-ray Diffraction	31
3.5.2. Fourier Transform Infrared Spectroscopy	31
3.5.3. UV-Vis Absorption Measurement	32
<b>3.6. Electrochemical Measurements</b>	<b>32</b>
3.6.1. Preparation of Modified Glass Carbon Electrode	32
3.6.2. Electrochemical Determination of Para-Nitrophenol	33
3.6.3. Analytical Performance of EGS/ZnO/GCE	33
3.6.4. Real Sample Analysis	34
3.6.5. Optimization of the Sensor	33
<b>4. RESULTS AND DISCUSSION</b>	<b>35</b>
<b>4.1. Structural Characterization of the Nanocomposites</b>	<b>35</b>
4.1.1. X-ray Diffraction	35
4.1.2. Fourier Transform Infrared Spectroscopy Analysis	37
4.1.3. UV- Visible Analysis	38
<b>4.2. Electrochemical Characterization of the Nanocomposites</b>	<b>40</b>

continues...

4.2.1. Electrochemical Characterization of the Various Modified Electrodes in Potassium Ferro Cyanide	40
4.2.2. Electrochemical Characterization of the Modified Electrode in 0.1M PBS	43
4.2. 3. Electrochemical Impedance Spectroscopy (EIS)	44
4.2.4. Cyclic Voltammetry Behavior of the Sensor in p-Nitrophenol	45
<b>4.3. Optimization of the EGS/ZnO/GC Electrode</b>	<b>48</b>
4.3.1. Effect of pH	48
4.3.2. Effect of Concentration	50
4.3.3. Effect of Interference	52
<b>4.4. Electrochemical Detection of p-Np under Optimized Parameters</b>	<b>53</b>
4.4.1. Reproducibility and Stability Test	55
<b>4.5. Determination of p-Nitrophenol in Waste Water using EGS/ZnO/GCE</b>	<b>55</b>
4.5.1. Recovery Test	56
<b>5. SUMMARY, CONCLUSIONS and RECOMMENDATIONS</b>	<b>58</b>
5.1. Summary and Conclusion	58
5.2. Recommendations	58
<b>6. REFERENCES</b>	<b>60</b>
<b>7. APPENDICES</b>	<b>66</b>

## LIST OF TABLES

<b>Table</b>	<b>Page</b>
1. Physical and Chemical properties of some phenol compounds	8
2. Different modified electrodes for the detection of p-nitrophenol	15
3. Average crystallite size (D) of as-synthesized Nanocomposites	36
4. Absorbance and maximum wavelengths of the as-synthesized nanoparticles	39
5. Detection of p-NP from the waste water sample	57

## LIST OF FIGURES

Figure	Page
1. Structure of some selected phenolic compounds	7
2. Structure of graphite oxide with some functional groups	18
3. Schematic of modified Hummers method for rGO preparation	20
4. (a) Excitation wave form of cyclic voltammetry (b) response obtained for the reversible cyclic voltammetry.	25
5. a) Excitation wave form of differential pulse Voltammetry. b) DPV response	27
6. XRD spectra of EGS, ZnO and EGS/ZnO nanocomposites	36
7. FTIR Spectra of a) EGS, b) ZnO and c) EGS/ZnO nanocomposites.	38
8. Uv-visible absorption spectra of EGS, ZnO, and EGS/ ZnO nanocomposites	40
9. CV of GCE in $K_3Fe(CN)_6$ at different scan rate ranging from 10 to 100 mV/s.	41
10. Cyclic voltammograms of a) GCE b) EGS/GCE c) ZnO/GCE d) EGS/ZnO/GCE	43
11. Cyclic voltammograms of a) GCE b) EGS/GCE c) ZnO/GCE d) EGS/ZnO/GCE	44
12. Impedance curve of the different modified electrodes in 0.1M of PBS	45
13. Cyclic voltammogram of the EGS/ZnO/GCE electrode in 0.1M PBS (pH 6.5) in the absence (a) and presence (b) of 0.1M p-NP.	46
14. Cyclic voltammograms of EGS/ZnO/GCE in 0.1M of PBS (pH 6.5) and 0.1M p-Np.	47
15. Cyclic voltammograms of a)GCE b)EGS/GCE c)ZnO/GCE d)EGS/ZnO/GCE in 0.1M PBS and in 0.1M p-NP at scan rates of 50mV/s.	48
16. Typical Cyclic voltammograms obtained at EGS/ZnO/GCE in various buffer solutions (pH 5 to 8) at the scan rate of 50 mVs.	49
17. Shows calibration curves at different pH values in PBS at concentration 0.1 M p- NP. 50	
18. Cyclic voltammograms of EGS/ZnO/GCE at different concentrations p-Np.	51
19. Calibration plot for current verse concentrations of p-NP	51
20. Cyclic voltammograms of EGS/ZnO/GCE with (a) no heavy metals, (b) lead metal (c) cadmium and (d) zinc metal concentration in 0.1 M of p-Nitrophenol	52
21. DPV voltammogram of standard solutions of p-NP (0.001- 2M) at pH 6.5, pulse amplitude 5 mV, pulse width 50 ms and scan rate 50 mV/ s.	54
22. Calibration plot of current verse concentrations of p-NP.	54

23. DPV of 2 M p-Nitrophenol concentration in industrial waste water sample a) standard solution b, c and d up on addition standard solution to the sample 56

## LIST OF TABLES IN APPENDIX

Tables in Appendix	Pages
1. Summary of electrochemical parameter for GCE evaluated from the CV of $K_3Fe(CN)_6$ at different scan rates	67
2. Summary of electrochemical parameters for the different nanoparticles evaluated for the CV of FCN at scan rate of 50 mV/s	67
3. Summary of electrochemical parameters for the different nanoparticles evaluated for the CV of 0.1 M PBS at scan rate of 50 mV/s	68

# Synthesis and Characterization of Extended Graphite Sheet/ZnO Nanocomposite Electrochemical Sensor for the Detection of Para-Nitrophenol

## ABSTRACT

*Extended graphite sheet (EGS) and EGS/ZnO was prepared by chemical reduction method and Zinc oxide (ZnO) was prepared by precipitation methods. The as prepared nanomaterials were characterized by Uv-Vis, FTIR and XRD techniques to identify the crystalline phase, molecular interaction, functional group and band gap energy determination respectively. The electrochemical properties of EGS, ZnO, EGS/ZnO modified glassy carbon electrode (GCE) was investigated using cyclic voltammetry(CV) and electrochemical impedance spectroscopy (EIS) in the presence of 2 mM  $K_3Fe(CN)_6$  + 0.1 M KCl and 0.1 M Phosphate buffer solution (PBS). The oxidation or reduction peaks of EGS, ZnO or EGS/ZnO modified GCE shows a slight increased after incorporating the nanomaterials at scan rates 50 mV/s. In the case of the EGS/ZnO nanocomposite the peak current enhanced due to the surface area and catalytic properties of graphite sheet and the conjugation of EGS to the ZnO nanoparticles enhanced the electron transfer. Therefore, EGS/ZnO/GCE was used as electrochemical sensor for the detection of para-nitrophenol in standard solution with differential pulse voltammetry (DPV). Effect of pH on EGS/ZnO/GCE sensor was optimized at (pH = 6.5) for the determination of para-nitrophenol. The electrode was applied for the determination of p-Np in standard solution of 0.001 to 2 M. The sensor results in linear range of 0.01 to 2 M ( $R^2 = 0.998$ ), limit of detection (LOD) was 0.00234 $\mu$ M and LOQ 0.0234 $\mu$ M with sensitivity of 0.00145 $\mu$ A $\mu$ M<sup>-1</sup>Cm<sup>-2</sup>. The sensor was used to determine the level of p-Np in industrial waste water and showed a good reproducibility, stability and low effect of interference with recovery of 99%. Therefore, the developed sensor could be a good candidate for the detection of p-Np in different samples.*

**Keywords:** Extended graphite sheet, Nanocomposites, Para-nitrophenol, Zinc oxide

## 1. INTRODUCTION

Phenolic compounds are a class of chemical compounds consisting of a hydroxyl functional group (OH) attached to the aromatic hydrocarbon group with a ring structure like that of benzene. These compounds have several applications indispensable in our daily life. They are in many ways similar to alcohols of aliphatic structures where the hydroxyl group is attached to a chain of carbons (Isensoy *et al.*, 2006).

These compounds are used extensively in industrial products, which can accumulate in the environment and the ecological food chain, via the consumption of these compounds by wildlife or uptake by plants and are widely presented in the atmosphere, water systems, and many food products. Industries where phenolic compounds appear, in the waste waters or else, include coal conversion, petroleum refining, pharmaceuticals, production of dyes, pesticides, surfactants, resins, and plastic (Lete, 2010). However, phenolic compounds such as alkyl phenols, nitrophenols, halogenated phenols butylated hydroxytoluene, alkylethoxy bisphenolic compounds, *p*-cresol, pyrocatechol, methylcatechol, chlorophenoxy etc are one of the popular pollutants of industrial wastes. Moreover, the compounds have high toxicity to the human organism when present above certain concentration in the environment (Jadwiga *et al.*, 2013). Especially thus industrial waste products are hazardous in developing countries like Ethiopia because such countries don't have the ability to recycle the industrial waste products.

Among these phenolic compounds, nitro phenols and their derivatives, those which are extensively used in the production of pharmaceuticals, leather production, synthetic dyes, and pesticides, are known to be serious environmental toxic, anthropogenic and biorefractory organic compounds which can cause serious damage to organisms and plants in the environment (Zhang *et al.*, 2012). Especially, nitrophenol (NP) isomers like *p*-nitrophenol (*p*-NP), *m*-nitro phenols and *o*-nitrophenol (*o*-NP) are found to be more toxic, and are of intense concern due to its high stability and solubility in water. Hence, they are regarded as one of the priority toxic pollutants by US Environmental Protection Agency (USEPA) (Yin *et al.*, 2010). From the above *para*-nitrophenolis considered to be a hazardous waste which has a high environmental impact due to its toxicity and persistence. Unfortunately, *p*-NP is widely used as intermediates in the production of pharmaceuticals, pesticides and dyestuffs, such as parathion insecticide which can also reversely hydrolyze

to form p-NP. Para-nitrophenol can also be used as leather fungicide and acid-base indicator. Based on this description, it is important to develop simple and reliable method for monitoring the amount of para-nitrophenol in various samples in the environments. Several instrumental techniques exist for the determination of organic pollutants, but are of less significance on the basis of efficiency and expense. Some of the various techniques that have been investigated to determine PNP, are fluorescence, high-performance liquid chromatography, capillary zone electrophoresis and spectroscopic method (Liu *et al.*, 2009).

However, a score of limitations are associated with these methods, including sample collection, tedious sample preparation, prolonged analysis time, and sophisticated and expensive instrumentation. Therefore, an alternative method such as electrochemical methods for monitoring para-nitrophenols has been developed as sensor technology which plays an important role in environmental safety and treatment. Thus for environmental and health safety, it is essential to produce simple, reliable, and inexpensive sensors for the detection of para-nitrophenol in the environment, because p-nitrophenols are hazardous and toxic pollutants with inhibitory and biorefractory nature and have a diverse effect on living organisms (Rahman *et al.*, 2011).

Among the sensor technologies, electrochemical methods have received considerable attention because of the advantage of fast response, cheap instrument, low cost, simple operation, time saving, high sensitivity and selectivity, real-time detection in situ condition. Until now, many electrochemical determination techniques mainly focus on utilizing the reduction of nitryl in p-NP, not the oxidation of hydroxide radical. Thus, the determination would be interfered by the oxygen molecule dissolved in solvent. Moreover, the reduction of nitryl is more complicated than the oxidation of hydroxide radical. Therefore, electrochemical determination of p-NP using the oxidation signal should be an appropriate alternative. Nevertheless, the use of bare electrode has revealed the drawback of weak electrochemical response and low sensitivity. Consequently, chemically modified electrodes (CMEs) have been widely investigated with various modification materials, especially nanophase materials, such as, gold nanoparticles,  $\text{TiO}_2$ , zeolite and

hydroxyapatite nano powder (HANP) etc. For example El Mhammedi *et al.* (2007) have evaluated the analytical performance of HA-NP-CPE for the detection of trace lead (II), paraquat and p-NP. Mohammed *et al.* (2017) made a simple, precise, ease to handle, low sample volume and highly sensitive chemical sensor for ultrasensitive determination p-NP. This sensor is based on perfect Ag<sub>2</sub>O nanoparticles decorated CNT deposited onto the GCE surface along with conducting coating binders at room conditions. Yang (2004) fabricated a single-wall carbon nanotubes (SWNT) film coated glassy carbon electrode (GCE) for the direct determination of para-nitrophenol .

In the past several years, coupled semiconductors formed by ZnO and other metal oxides or sulfides such as TiO<sub>2</sub>, SnO<sub>2</sub>, Fe<sub>2</sub>O<sub>3</sub>, WO<sub>3</sub>, CdS, ZnS, CuO and so on, have been reported. The results showed that coupling of different semiconductor oxides can reduce its band gap (Chao *et al.*, 2010). From this zinc oxide (ZnO) has been explored to modify electrodes for electrochemical detection of p-NP due to its wide electrochemical potential window, well known II-IV semiconductor, versatile material, wide band gap, large excitation binding energy, low reactivity to the electrochemical reactions and the presence of surface defect along with its low cost(Wang *et al.*, 2009). Moreover, among the several carbon based nanomaterial electrodes such as carbon paste, carbon nanotubes and reduced graphene, extended graphite sheet electrodes have been extensively used in electrochemical detection of p-NP because of its wide potential window, very thin, good electron transport properties and high effective surface area.

Based on the exceptional individual properties of both extended graphite sheet and ZnO as an electrode material, the resulting composites of both of them may display unique sensing properties of environmental pollutants like para-nitrophenol due to the synergistic effect between them for enhanced electrochemical performance. There are many synthesis methods to combine extended graphite sheets and ZnO nanoparticles such as thermal decomposition (Zhu *et al.*, 2006), electrochemical route (Palanisamy *et al.*, 2012), ultrasonic spray pyrolysis (Lu *et al.*, 2010), electro hydrodynamic atomization and solvothermal process (Wu *et al.*, 2010). However, most of the attempts in the synthesis of a graphene sheet/ZnO nanocomposite involved is a chemical reduction method and precipitation

method which involves the reduction of graphene oxide and an in-situ growth of ZnO which culminate in the presence of an oxygenated functional group on the graphene surface and impurities in the composite due to an incomplete reduction and purification process. So, extended graphite sheet/ZnO nanocomposite may be a suitable electrode modified material for pollution detection and determination.

To the best of authors knowledge, there are no previous report available on electrochemical detection of p NP based on extended graphite sheet/ZnO nanocomposites modified electrode. Moreover, p-NP is extremely toxic, and usually serious to both health and environment, therefore, it is immediately required to develop an efficient sensing material as well as sensing method for the detection of p-NP. In this approach, for the first time is made EGS/ZnO nanocomposite chemical sensor for the determination p-NP. This sensor is based on perfect graphite sheet nanoparticles chemically reduced ZnO NCs deposited onto the GCE which tested for the detection of para nitro phenol in industrial waste water. Our motivation is that commonly toxic chemical from industrial wastes like leather industries are harmful to the environment particularly in Ethiopia because the waste products are not recycled as raw material for other industries for further uses. Therefore, differential pulse voltammetry (DPV) was used for the determination of p-NP since DPV is often used to detect extremely low concentration of chemicals because in these measurements, the effect of the charging current is minimized, and thus high sensitivity can be achieved.

## Objective of the Study

### General Objective

- To develop a sensitive electrochemical sensor for the detection of para- nitrophenol using extended graphite sheet/ZnO nanocomposite.

### Specific Objectives

- To synthesize extended graphite sheet NPs, ZnONPs and extended graphite sheet/ZnO nanomaterials by using chemical reduction method and precipitation method.
- To characterize the above as-synthesized nanomaterials by using modern instruments such as XRD, UV-Vis and FTIR techniques.
- To evaluate the chemical performance of the extended graphite Sheet /ZnO using CV and EIS.
- To optimize the parameters such as pH of solution and concentration of substrate.
- To evaluate the electrochemical properties of p-nitrophenol on the unmodified and modified electrode surface by using cyclic voltammeter (CV) and Differential pulse voltammetry (DPV).
- To evaluate the extended graphite sheet/ZnO nanocomposite electrochemical sensor for the detection of Para- nitrophenol.
- To determine the p-nitrophenol concentration in industrial waste water (leather industry).

## 2. LITERATURE REVIEW

### 2.1. Phenolic Compounds

Studies of phenolic compounds have dramatically increased during the past few decades due to the unique and remarkable properties of the compounds in biological and environmental systems, Such as plants and human beings as well as in non-biological systems such as foods. The basic structural building block of all phenolic compounds is a phenyl ring bearing a hydroxyl group, this unique structure allows them to be either hydrogen-donors or acceptors. Thus, phenolic compounds exhibit antioxidant properties due to their ability to scavenge free radicals generated from lipids, proteins, and oligonucleic acids. The free radical scavenging ability of phenolic compounds has been widely studied and associated with multiple biological effects including health benefits for human beings (Yao *et al.*, 2004).

Nitro phenols like p-nitro phenols are among the class of phenolic compounds which consist of a phenol molecule with one or more nitro-groups attached to the aromatic ring. The term is most often used to describe singly nitrated phenols and is among the most common organics of toxic persistent pollutants in industrial and agricultural environments. The presence of an acceptor for protons (the nitro group) and a donor for protons (the OH group) on the same molecule may affect the structure of the molecule as well as the molecular arrangement in the solid state.

Phenolic compounds are used as raw material in the manufacture of a wide range of important chemicals including phenolic resins, bisphenol, caprolactam, alkylphenols and adipic acid. Phenolics are also widely used for the treatment of injuries for making aspirin drug also as antiseptics and local anaesthetics. It is suitable in the manufacture of paints and varnish removers, lacquers, rubber, ink, and illuminating gases, tanning dyes, perfumes, toys and soaps. Moreover, as an industrial chemical in the manufacturing of certain products such as “resins, plastics, fibers, adhesives, iron, steel, aluminum, leather, and rubber”, present in disinfectants, cigarette smoke, and emissions from, in household

products and industrial synthesis, as disinfectants in household cleaners, lotions, salves, and in mouth wash (Wade, 1999). Some of the different structure phenolic compounds are shown in Figure 1 (Dionex Corporation, 2008).

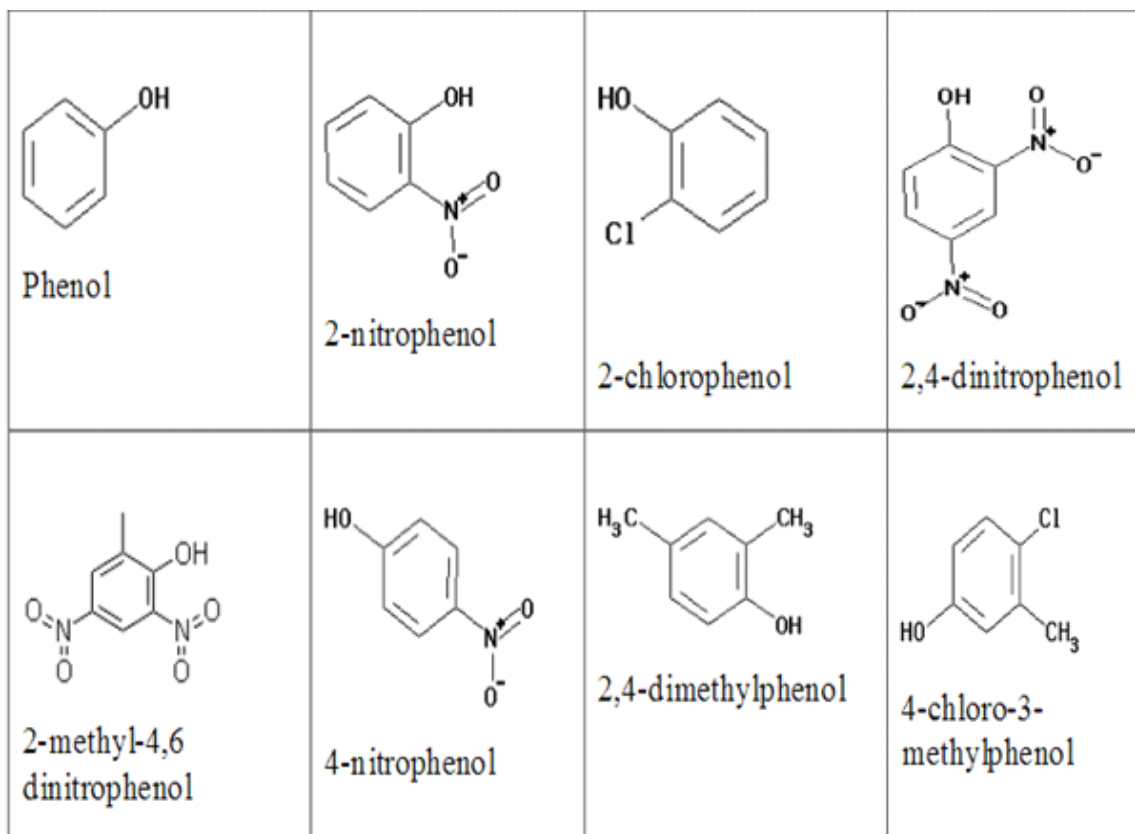


Figure 1. Structure of some selected phenolic compounds

Phenol and its compounds have a low melting point; it crystallizes in colorless prisms and has a characteristic of slightly pungent odor. In the molten state, it is a clear, colorless, mobile liquid. In the temperature range  $T < 68.4\text{ }^{\circ}\text{C}$  its miscibility with water is limited; above this temperature it is completely miscible. The melting and solidification points of phenol are quite substantially lowered by water. Phenol is readily soluble in most organic solvents (aromatic hydrocarbons, alcohols, ketones, ethers, acids, halogenated hydrocarbons etc.) and somewhat less soluble in aliphatic hydrocarbons. Phenol forms azeotropic mixtures with water and other substances and some other properties of some phenol compounds are shown in the Table 1 (Merck Chemicals, 2010).

Table 1. Physical and chemical properties of some phenol compounds

	<b>Formula</b>	<b>Molar mass (g/mol)</b>	<b>Melting point (°C)</b>	<b>Boiling point (°C)</b>	<b>Density (g/cm<sup>3</sup>)</b>
Phenol	C <sub>6</sub> H <sub>5</sub> OH	94.11	40.8	181.8	1.06 (20 °C)
2-nitrophenol	2-(NO <sub>2</sub> )C <sub>6</sub> H <sub>4</sub> OH	139.11	43 - 45	215 - 216	1.26 (20 °C)
2-chlorophenol	2-(Cl)C <sub>6</sub> H <sub>4</sub> OH	128.55	7	174	1.26 g (20 °C)
2,4-dinitrophenol	2,4-DNP	184.11	114 - 115		1.68 (20 °C)
2-methyl-4,6-dinitrophenol	C <sub>7</sub> H <sub>6</sub> N <sub>2</sub> O <sub>5</sub>	198.14	82 - 85	312	
4-nitrophenol	O <sub>2</sub> NC <sub>6</sub> H <sub>4</sub> OH	139.11	110 - 115	279	1.48 (20 °C)
2,4-dimethylphenol	2,4-(CH <sub>3</sub> ) <sub>2</sub> C <sub>6</sub> H <sub>3</sub> OH	122.16	25	211	1.016 (25 °C)
4-chloro-3-methylphenol	4-(Cl)-3-(CH <sub>3</sub> )C <sub>6</sub> H <sub>3</sub> OH	142.58	63 - 65	235 - 239	1.37 (20 °C)
2,4,6-trichlorophenol	C <sub>6</sub> H <sub>3</sub> Cl <sub>3</sub> O	197.44	65 - 68	244 - 246	1.675 (25 °C)
2,4-dichlorophenol	2,4-(Cl) <sub>2</sub> C <sub>6</sub> H <sub>3</sub> OH	163	40 - 43	209 - 211	

## 2.2. Environmental Pollution by Phenolic Compounds

Wide use of phenol and its derivatives led to studies of its occupational exposure and toxicity. Phenol toxicity in humans is not a big surprise, as this compound is toxic to most microorganisms, which explains its common use as a general disinfectant. This fact complicates treatment of phenol containing wastewater by conventional biological process (Khan *et al.*, 1985). Phenol compounds are of the popular pollutants of industrial wastes

and moreover, the compounds have high toxicity to the human organism when present above certain concentration limits this requires rapid determination of these compounds. They can be easily absorbed by animals and humans through the skin and mucous membranes that affect many organs, such as primarily lungs, liver, kidneys, and genitourinary system and are also toxic to plants. Many of them are also known for persistence in environment, reacting with chlorine during water treatment, and biomagnifications. Due to their presence in water, air and food matrices, they represent significant toxic risks to the environment and human health (Silva *et al.*, 2014).

Nitrophenols like para-nitro phenols are among the most common organics of toxic persistent pollutants in industrial and agricultural wastewater. They are considered to be hazardous wastes and priority toxic pollutants by U. S. Environmental protection Agency (EPA). They are present in industrial effluents of chemical plants producing pesticides, explosives, dyestuffs, and products for leather treatment and in the agricultural irrigation effluents. Moreover, they were also found in rainwater, in Germany, in concentrations up to 170 nM which are formed in the troposphere by the interaction of mono aromatic chemicals with nitrogen oxides and ozone. Purification of wastewater polluted with para-nitrophenol (p-NP) is a very difficult task. The presence of a nitro group in the aromatic ring enhances the stability to chemical and biological degradation. These pollutants are unaffected by aerobic biodegradation while the anaerobic degradation produces nitroso and hydroxylamine compounds which are known as carcinogenic (Megharajet *et al.*, 1991).

In Ethiopia Pollution of water and other environment by toxic and non biodegradable organic materials of industrial or agricultural origin, like pesticides, brings about very serious health hazards for all living species of the nature. The enormous diversity of pollutants of different chemical composition excludes the possibility of using a universal treatment method and led to the development of special treatment methods for water decontamination. Among the pollutants a class of phenol compounds even though has played a considerable role in agriculture because of their high insecticidal activity, but they can cause irreversible damage to organisms and plants even at very low concentration. Among them, p-Nitrophenol (p-NP) is breakdown product as well as a chemical intermediate in the production of

organophosphorus insecticide derivatives of parathion. Therefore, it is of great importance to develop methods for the determination of p-NP in terms of environmental protection and food security.

## **2.3. Method of Determination of Phenolic Compounds**

There are several methods which have been developed over the years for the determination of nitro phenol compounds in waste water. Some of these methods are spectrophotometer, electrochemical methods, capillary electrophoresis, the gas chromatographic (GC) method using liquid-liquid extraction and either using flame ionization detection (FID) or derivatization and electron capture detection (ECD) to analyze different phenols at a low concentration (Eaton *et al.*, 2005).

### **2.3.1. Spectroscopic and Chromatographic Determination**

Spectrophotometer is one of the relatively simple techniques for quantification of phenolic compounds. It is the study of the interaction between matter and electromagnetic radiation. Historically, spectroscopy originated through the study of visible light dispersed according to its wavelength by a prism. Later the concept was expanded greatly to include any interaction with radiative energy as a function of its wavelength or frequency. Spectroscopic data is often represented by an emission spectrum, a plot of the response of nitro phenol as a function of wavelength or frequency. It occurs when energy from the radiative source is absorbed by the phenolic compound then absorption is often determined by measuring the fraction of energy transmitted through the material and the absorption decreases the transmitted portion. But the methods are easily interfered by related compounds (Crouch *et al.*, 2007).

In our present time, there is a rising interest in applying high performance liquid chromatography (HPLC) which is not subject to temperature dependence to the determination of not just volatile organic compounds like aliphatic and polyaromatic hydrocarbons, saturated and unsaturated aliphatic halogen compounds, halo forms and some esters, phenols unlike the gas chromatography, but for all organic and inorganic

matter present in water samples. Hence, in liquid chromatography, a liquid passes the porous solid stationary phase and the elute flows through a detector. In HPLC, the mobile phase is pumped at high pressure and this need high cost to buy columns and waste more organic solvents (Crompton, 1999).

Capillary electrophoresis (CE) is the other high-resolution technique conducted with a solution of ions in a narrow capillary column. It is suitable to identify charged low and medium-molecular weight compounds rapidly and efficiently with high-resolution and has low sample and reagent volume requirements. There are few studies on the use of CE to separate and identify phenolics in plant materials. Capillary electro chromatography (CEC) and capillary zone electrophoresis (CZE) coupled with ultraviolet detection (UV), and electrochemistry detection or mass spectrometry detection (MS) are the most widely used techniques among the different types of CE separation. They need high cost to buy columns and waste more organic solvents (Wang *et al.*, 2010).

Gas chromatography (GC) is also applied for the separation, identification and quantification of phenolic compounds such as phenolic acids, nitro phenols, condensed tannins and flavonoids etc. The major concerns of GC analysis, that are not applicable to HPLC techniques, are the derivatization and volatility of phenolic compounds. With GC quantification of phenolics from food matrices may involve clean-up steps such as lipid removal from the extract, release of phenolics from the glycoside and ester bonds in enzymatic, alkaline and acidic media and chemical modification steps, such as transformation to more volatile derivatives. There are a several types of reagents used to modify and create volatile derivatives. GC methods can sometimes require relatively expensive reagents and need derivatization before analysis and it cannot be used directly to aqueous samples (Eaton *et al.*, 2005).

### **2.3.2. Electrochemical Methods of Determination of Phenol Compounds**

As mentioned in the above Phenol and substituted phenols like nitro phenols are among the most toxic substances and are widely distributed in industrial and natural wastes. Therefore, the sensing of nitro aromatic compounds is of great importance to evaluate the

risk of different environmental samples such as wastewater from mining, paint, pesticides, insecticides, leather and pharmaceutical industries, petrochemical products. p-Nitrophenols pollutants are among the harmful to environment due to their high toxic potential level for humans, animals and plants which have been included in the priority lists of monitored pollutants in many countries (Busca *et al.*, 2008). The p-Nitrophenols' detriment and vast scale distributions in the ecological environment. The detection of them has become one of the important studies of environmental analysis. The emerging nanotechnology has opened up new exciting avenues for offering great opportunities for analytical applications, mostly due to the extraordinary physical and chemical properties of nanostructure materials (Liu *et al.*, 2007; Liu *et al.*, 2008).

Therefore, electrochemical techniques are being developed and improved for determination of phenolic compounds. These techniques are low-cost, sensitive and enable rapid analysis of sample. They can be applied in analysis of samples without the necessity of modification. It is possible to determine and quantify phenolic compounds in highly complex biological matrices. Analysis can be performed in a stationary system using techniques such as differential pulse voltammetry, cyclic voltammetry or biosensor applications based on enzyme catalysis. In addition to stationary systems, dynamic systems based on voltammetry or amperometry are commonly used in electrochemical analyzing of phenolic compounds. Electro analytical techniques are advantageous in the detection of phenolic compounds (Dejmkova *et al.*, 2009). This can be divided into several classes, Potentiostatic methods operate at a constant potential of the working electrode (amperometry and potentiostatic coulometry) and amperostatic methods (amperostatic voltammetry and coulometry) operate at a constant current. Coulometric detector, which measures the electrical charge required to oxidize or reduce the total amount of the compound during its pass a cell of detector, is predominantly used for the determination of phenolic compounds (Vallset *et al.*, 2009).

## 2.4. Chemical Sensors

Sensors are the devices, which are composed of an active sensing material with a signal transducer. The role of these two important components in sensors is to transmit the signal without any amplification from a selective compound or from change in a reaction. These devices produce any one of the signals as electrical, thermal or optical output signals which could be converted in to digital signals for further processing (Sakaguchi *et al.*, 2007). A small device used for direct measurement of a physical quantity of an analyte in a sample matrix and the response is continuous and reversible. Chemical Sensors (detectors/transducers) covers a wide category of devices used to monitor, measure, test, analyses data as generated due to changes in a measured norm (usually concentration for chemical sensors). One of the ways of classifying sensors is done based on output signals (Guinovart *et al.*, 2013).

## 2.5. Electrochemical Sensor

Electrochemical sensor is a small device used for direct measurement of a physical quantity of an analyte in a sample matrix. Electrochemical sensor consists of a transduction element covered by a recognition layer which may be chemical or biological materials. The recognition layer interacts with target analyte and then transduction element translates the chemical changes into electrical signals. Therefore, electrochemical sensor produces an electrical signal that is related to the concentration of an analyte. Electrochemical sensor produces an electrical signal that is related to the concentration of an analyte but in biosensor biological recognition processes are converted into quantitative amperometric or potentiometric response (Chung *et al.*, 2008). Electrochemical sensors have more advantages over the others due to the electrodes of electrochemical can sense the materials which are present within the host without doing any damage to the host system and produces an electrical signal that is related to the concentration of an analyte. Electrodes usually modify with surface active layers such as conductive polymers, inorganic oxides or hybrid materials in the area of electrochemistry research. A number of reviews discussing the preparation, characterization, and electrochemical behavior of chemically modified

electrodes are available. One of the interesting application areas of modified electrodes are in sensors.

## **2.6. Working Principle for Detecting of Para-Nitrophenol**

### **2.6.1. Chemically Modified Electrodes**

Since the electrode fouling during the electrochemical analysis or disposal of phenolic compounds was a common problem, many efforts have been made in order to alleviate this problem. Introduction of functional interfaces for electrode surface modification was an important approach. These functional interfaces were expected to prevent polymeric substrates from adsorbing onto the surface of electrode, or form soluble complexes with polymeric substrates as shown in Table 2.

The CMEs represent a modern approach to electrode systems. These electrodes rely on the placement of reagent on the surface to impart the behavior of reagent to the surface of the electrode. Such deliberate alteration of the electrode surfaces can thus meet to the need of many electro analytical problems and may form basis for new analytical applications including energy conversion, electrochemical synthesis and microelectronic devices. CME is that generally quite thin film from a molecular monolayer to perhaps a few micrometers-thick multilayer's. Electrodes are usually chemically modified chemisorptions-adsorption, covalent bonding and polymer film coating composite etc.

Table 2. Different modified electrodes for the detection of p-phenol

Electrode	Linear dynamic range( $\mu\text{M}$ )	Limit of detection ( $\mu\text{M}$ )	Sensitivity ( $\mu\text{A}\mu\text{M}^{-1}\text{Cm}^{-2}$ )	Reference
Apatite/CPE	0.2-100	0.03023	0.0062	(Elmahammed <i>et al.</i> , 2009)
MWCNT/GCE	2-400	0.4	-	(Luo <i>et al.</i> , 2008)
OMCs/GCE	2-90	0.1	-	(Zhang <i>et al.</i> , 2013)
GO/GCE	1-120	0.02	0.035	(yang <i>et al.</i> , 2011)
chitosan/GCE	0.2-550	0.057	0.033	(Yin <i>et al.</i> , 2011)
SWCNT/GCE	0.01-5	0.0025	-	(Yang <i>et al.</i> , 2004)
Nano-gold/GCE	10-1000	8	-	(Chu <i>et al.</i> , 2010)
Ionic liquid/CPE	3-800	0.7	0.031	(Sun <i>et al.</i> , 2008)
Nano $\text{CuO}_2/\text{Pt}$	10-1000	0.1	1.396	(Guet <i>et al.</i> , 2010)

## 2.7. Nanomaterials For Modified Electrode

### 2.7.1. Nanoparticles

Nanoparticles (Nps) are the nanometer-sized solid particles engineered at atomic or molecular scale so as to form either novel or superior physical properties that are not attainable by conventional bulk solids. From theoretical point of view, nanoparticles are frequently called Nano clusters or simply clusters which are defined as the combination of

millions of atoms or molecules (Fernando *et al.*, 2008). These atoms or molecules may be of same or of different kind. Nanoparticles can be of amorphous or crystalline form and their surfaces can act as a carrier for liquid droplets or gases. Nanoparticles can be synthesized using two techniques: top-down approach and bottom-up approach. In top-down approach, the bulk materials are broken down to the nanoparticles; however, in bottom-up approach, the nanoparticles combine so as to form the bulk material. The bottom-up approach is more convenient than that of the top-down approach because in the later, the chances of contamination are quite high. Nanoparticles are of great importance in our day to day life and form the basis of nanotechnology. These are used in different forms depending upon the type of applications.

### **2.7.2. Bimetallic Nanoparticles**

Bimetallic nanoparticles are composed of two different metals have drawn a greater interest than the monometallic nanoparticles from both scientific as well as technological point of view Constituting metals and their nanometric size determine the properties of the bimetallic nanoparticles. These are synthesized by the combination of different architectures of metallic nanoparticles. They actually offer us the tendency of optimizing the energy of Plasmon absorption band of metallic mixture which offers us a multipurpose tool for biosensing. These properties may differ from those of pure elemental particles and include unique size dependent optical, electronic, thermal and catalytic effects. In bimetallic catalysts, the electronic effect plays an important role which describes the charge transfer. Alloying of the constituting elements can result in the structural changes of the bimetallic nanoparticles. From monometallic to bimetallic nanoparticles, an extra degree of freedom is introduced (Sharma *et al.*, 2015).

### **2.7. 3.Metal Oxides Nanoparticles**

Nanostructured metal oxide or semiconductors were extensively applied to energy and environment field due to their nontoxicity, good biocompatibility, high surface area, catalytic activity enhanced electron transfer kinetics and chemical stability. Moreover, nanometal oxides could provide biocompatible electro active surface beneficial for

immobilizing biomolecules which further enhance the ability of biological recognition materials (Srivastava *et al.*, 2011). Recently, metal oxides can offer promising electro active materials due to enhancement of the electrochemical reversible redox reaction, wide potential window and large surface to volume ratio. The nanostructures of metal oxide semiconductors are attractive and important for nanosensors research because of their practical and theoretical importance in biological, environmental science and analytical chemistry applications.

Among these metal oxides, ZnO, CuO and NiO have different and attractive morphologies as nanowires, nanorods (NRs), nanotubes, nanoleaves, nanoflowers, etc, that make them useful to fabricate nano devices for optoelectronic and sensing applications. ZnO nanostructure have become increasingly popular, because of the different morphologies grown by various growth methods including the vapor-liquid-solid, chemical vapor deposition, electrochemical deposition and hydrothermal methods. Among various metal oxides, zinc oxide (ZnO) is an exceptional material with high specific surface area, non toxicity, chemical stability, electrochemical activity, and high electron communication features. Thus great interested properties of ZnO have role in sensor construction (Huang *et al.*, 2001). Recently, metal oxides can offer promising electro active materials due to enhancement to the electrochemical reversible redox reaction, wide potential window and large surface-volume ratio.

#### **2.7.4. Carbon Nanomaterials**

Bimetallic nanocomposites supported on carbon are of great interest. Carbon supported bimetallic nanoparticles have reduced surface area which enhances their properties to a large extent. Water contamination is one of the major problems faced by human beings now a days. The presence of unwanted material, ions, micro-organisms such as fungi, bacteria and virus, etc contaminates the water. The presence of per chlorate ion makes the water unsafe for drinking. Nanotechnology provides an alternate to the water purification. When ruthenium-palladium bimetallic nanoparticles are supported on the carbon matrix, they efficiently reduce the per chlorate into chloride ions under acidic conditions and thus,

helps in treating waste or contaminated water containing per chlorate as the major impurity (Liu *et al.*, 2013).

### 2.7.5. Graphene Oxide

Graphene oxide is a lined two-dimensional carbon sheet with diverse oxygenated functional groups which has a thickness around 1 nm and lateral dimension of few nanometers to several microns. The history of GO was begun by the British chemist B.C. Brodie in 1859. It is a cheapest precursor to produce process able graphene in high quantity and is the most suitable starting material for synthesis of functionalized graphene and then graphite sheet. The exact structure of GO is difficult to describe precisely due to the complexity of the material, its amorphous, berthollide character (nonstoichiometric atomic composition) and the lack of precise analytical techniques for the characterization of GO (Dreyer *et al.*, 2010).

Despite of those difficulties, most of the models proposed so far have described it as a poly dispersed material with a structural formula. The intrinsic property of the functional groups (i.e., hydroxyl, epoxy, lactol, carbonyl, carboxylic acid and organosulfonate) in GO is highly influenced by the synthesis conditions like reaction time, temperature and procedures of synthesis. Hydroxyl and epoxy groups destroy localized  $\pi$  electrons and results in decreasing carrier mobility and its electrical conductivity which both make it an insulating material (a sheet resistance) (Gilje *et al.*, 2007) and the Sheet resistance is the measure of the electrical conductance of the sheet independent of its thickness.



Figure 2. Structure of graphite oxide with some functional groups

### 2.7.6. Reduced Graphite Oxide

Reduced graphite oxide is one kind of chemically derived graphene and it can be also named as functionalized graphene, chemically modified graphene, chemically converted graphene, or reduced graphene. It is a 2D form of carbon but with chemical moieties that render new functionalities while preserving some properties of pristine material. The chemical exfoliation of graphite through oxidation leads to covalent functionalization followed by reduction which brings reduced graphene oxide. This sequenced process noticeably changes the structure of graphene. Therefore, rGO is not exactly the same as graphene because of the difference in their intrinsic properties (Eda, 2010).

Even though the relativistic intrinsic properties like charge carrier mobility and conductivity observed in ideal graphene are absent in rGO, flexible process ability and versatile properties make rGO interesting in fundamental research as well as application in energy storage. Therefore, due to its ease of processing and unique properties such as mechanical stability, tunable electrical and optical properties, rGO based-thin films provide great hopes for their use in electronic and opto-electronic, where in components are built on plastic or paper like platforms, electrodes, ultra capacitors (Stoller *et al.*, 2008). The quality of graphene produced depends on the process parameters used when reducing graphene oxide (GO) and rGO is synthesized as shown in the Figure 3 (Giljeet *et al.*, 2007).

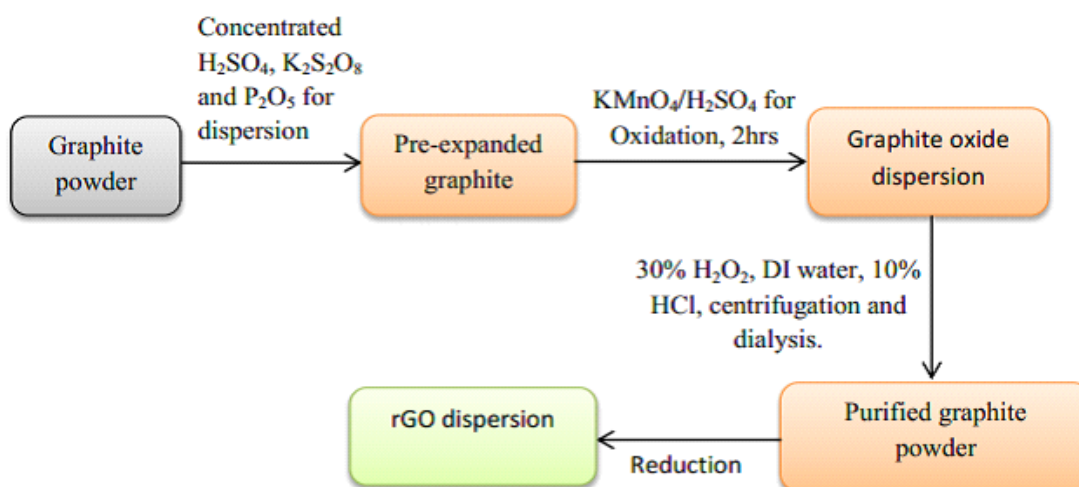


Figure 3. Schematic of modified Hummers method for rGO preparation

### 2.7.7. Carbon Nanotubes

Carbon nanotubes (CNTs) are seamless cylinder-shaped macromolecules with a radius as small as a few nanometers, and up to several micrometers in length. The walls of these tubes are constructed of a hexagonal lattice of carbon atoms and capped by fullerene-like structures. Carbon nanotubes are large macromolecules that are unique for their size, shape, and remarkable physical properties like excellent electronic properties, good chemical stability and large surface areas. They can be thought of as a sheet of graphite (a hexagonal lattice of carbon) rolled into a cylinder. Currently, the physical properties are still being discovered and disputed. What makes it so difficult is that nanotubes have a very broad range of electronic, thermal, and structural properties that change depending on the different kinds of nanotubes (defined by its diameter, length, and chirality) (Coleman *et al.*, 2006). The unique structure of CNTs can be divided mainly into multi-walled carbon nanotubes (MWCNTs) and single-walled carbon nanotubes (SWCNTs).

MWCNTs are composed of two or more concentric cylindrical shells of graphene sheets coaxially arranged around a central hollow area with spacing between the layers. In contrast, SWCNTs are made of a single cylinder graphite sheet held together by Vander Waals bonds (Daniel *et al.*, 2007).

## **2.8. Methods of Synthesis of Nanoparticles**

Researchers have discovered many new methods to prepare nanoparticles which are of the required size, composition and shape because these factors greatly influence the properties of the material. Some of the methods used for the synthesis of the nanoparticles are discussed below.

### **2.8.1. Electrochemical Reduction**

In this method, electricity is used as the driving or controlling force. The electric current is passed between the two electrodes which are separated by electrolyte (Katwal *et al.*, 2015). Researchers used electrochemical method for the preparation of metallic nanoparticles. They dissolved the metallic anodic sheet and metallic salt formed was reduced by the cathode to metallic particles. Merits of electrochemical technique include low cost, high purity of particles, particles size control by optimizing the current density and simple method of operation. This method is mainly used in industrial applications.

### **2.8.2. Sol-Gel Reaction Method**

The sol-gel method derives from two words; sol and gel. The sol is a stable suspension of colloidal solid particle in liquid. The dispersed phase in sol is so small that there only Vander-Waal force. In gel, the concentration of solid is more than liquid. It is a semi-rigid mass in which the particles or ions left after the evaporation starts to form a continuous network. In most of the gel systems, there exist the covalent interactions. The combination of these two network functions is called sol-gel method. This method mainly consists of two main reactions, hydrolysis and condensation. Various bimetallic NPs are synthesized by sol-gel method, such as Au-Ag, Au-Pd and Au-Pt, etc. This method is quite useful because it is a simple, economic and effective method to produce good quality nanoparticles (Sharma *et al.*, 2016). It is quite interesting since it is a low temperature technique that offers the ability to control the product's chemical composition.

### **2.8.3. Chemical Precipitation Method**

Chemical precipitation is the process of conversion of a solution into solid by converting the substance into insoluble form or by making the solution a super saturated one. It involves the addition of chemical reagents and then separation of precipitates from the solution (Sharma *et al.*, 2016). Nanoparticles of ZnO and ZnS can be prepared by this method. Since it is a single step process and helps in large scale production of nanoparticles without any impurities, it is quite a useful technique. It even helps in the purification of water and is long produces permanent results.

### **2.8.4. Hydrothermal Method**

In this method, nanoparticles are produced under the influence of high temperature, about 470°C and pressure, below 300 Mpa. This method allows the dilution of components which are normally non-soluble under normal conditions. The properties of the resulting nanoparticles then depend upon the pH, temperature and pressure of the medium. Further enhancement in this method can be useful because it will help in monitoring the crystal growth. This method is advantageous due to the production of high yield and pure products. In addition to this, it produces crystals of high quality and offers us the ability to control the physical and chemical properties of the resulting nanoparticles. Disadvantages of this method include the high equipment cost and it is not possible to monitor the growth process of crystal. Zeolites and nanoparticles of Lead telluride have been synthesized by this method.

### **2.8.5. Impregnation Method**

Catalyst support is the material, usually a solid with a high surface area, to which a catalyst is affixed. The activity of heterogeneous catalysts and nanomaterial-based catalysts occurs at the surface atoms. Consequently, great effort is made to maximize the surface area of a catalyst by distributing it over the support. The support may be inert or participate in the catalytic reactions. Typical supports include various kinds of carbon, alumina, silica and organic polymer. In impregnation techniques, the support is contacted with a precursor

solution, in other word impregnation is related to ion exchange (adsorption processes) and the interaction with the support is dominant. Thus, low loadings, often for precious metals, are achieved by adsorption of the precursor molecules onto surface groups of the support (ion adsorption) or through the exchange of ions in, for example, zeolites (ion exchange), after which excess precursor is removed. When higher loadings are required, the washing step is skipped and the support is directly dried, so that all precursor ends up on the support (impregnation and drying). Impregnation can be performed to incipient wetness, whereby the pores of the support are filled with precursor solution, to prevent deposition on the external surface of the catalyst grains and to limit waste (Munnik *et al.*, 2015).

### **2.8.6. Chemical Reduction Method**

This is the preparation method for the synthesis of metalnanoparticles such as the material chemical reduction in aqueous medium into the interlayer space with various polymersurfactants or reducing agents. In this method, nanoparticles are produced under the influence of heat, filtration, dissolution and centrifugation. Chemical reduction method is applicable in soft matrixes swelling and ion exchange properties. Its interlayer space has been used for the synthesis of nanoparticles materials and biomaterials, as support for anchoring transition-metal complex catalysts and as adsorbents (Mansor *et al.*, 2009).

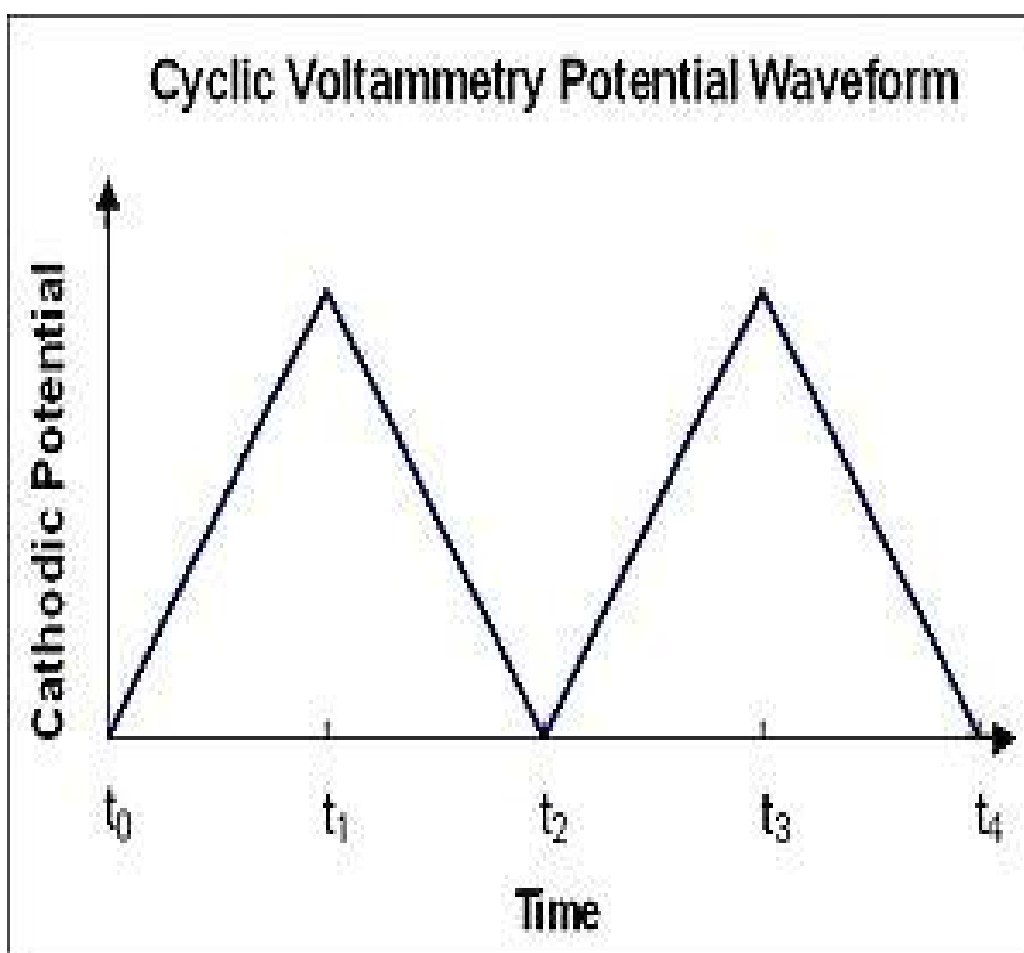
## **2.9. Electrochemical Techniques**

### **2.9.1. Cyclic Voltammetry**

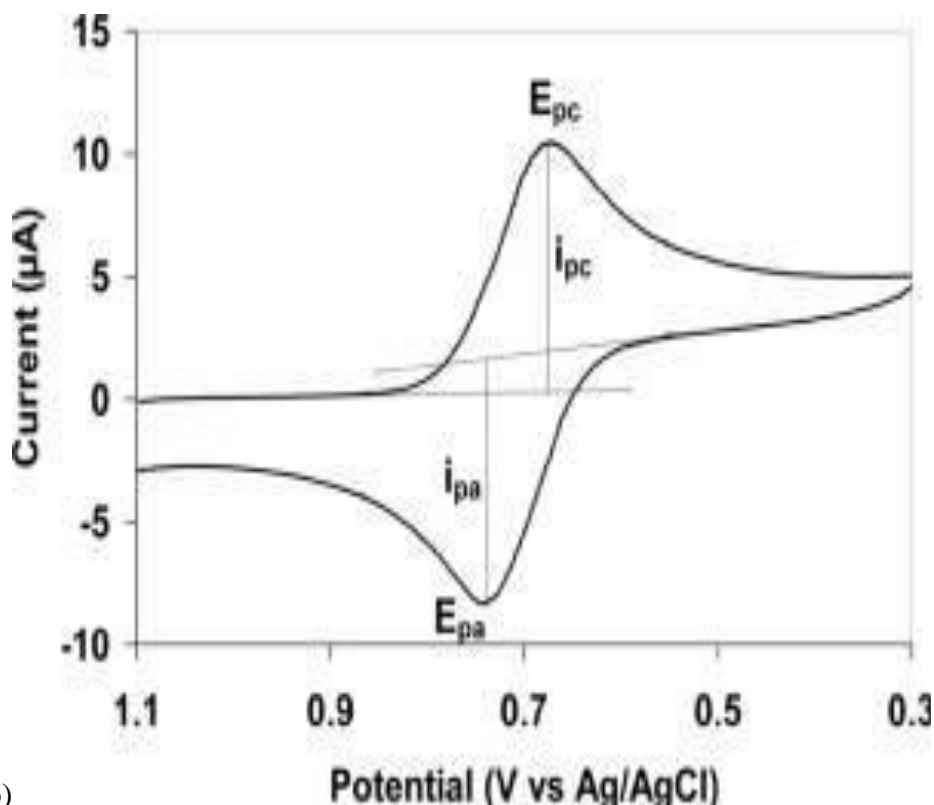
Cyclic voltammetry (CV) consists of the most effective and versatile electro analytical technique for the study of electro active species. Its versatility was combined with ease of the measurement has resulted in extensive use cyclic voltammetry in the field of electrochemistry. The effectiveness of cyclic voltammetry results from its capability for rapid observing redox behavior over a wide potential range (Bard *et al.*, 2001). It is most widely used techniques of all methods by both electrochemist and non electrochemist. It allows the analyst to mechanistically study systems, especially the assignment and characterization of redox couples. Cyclic voltammetry consists of cycling potential of an

electrode, which is immersed in unstirred solution and measuring the resulting current as shown in Figure 4.

The potential of the working electrode is controlled versus a reference electrode such Ag/AgCl/KCl and the controlling potential that is applied across these two electrodes can be considered an excitation signal. The excitation signal for cyclic voltammetry is linear potential scan with a triangular wave form as shown in Figure 4. This triangular potential excitation signal sweeps the potential of the electrode between two electrode sometimes called the switching potential (Bard *et al.*,2001).



a)



b)

Figure 4.(a) Excitation wave form of cyclic voltammetry (b) response obtained for the reversible cyclic voltammetry.

A cyclic voltammogram is obtained by measuring the current at the working electrode during the potential scan. The current can be measured considered as the response signal to the potential excitation signal. The voltammogram is a display of current (vertical axis) versus potential (horizontal axis). Because the potential varies linearly with time, the horizontal axis can also be thought as time axis. Cyclic voltammetry has become an important and widely used electro analytical technique in many area of chemistry. It is rarely use for quantitative determinations, but it is widely used for the study of redox process, for understanding reaction intermediate, and obtaining stability of reaction products. The important parameter of a cyclic voltammogram are the magnitude of the anodic peak current ( $i_{pa}$ ), cathodic peak current ( $i_{pc}$ ), anodic peak potential ( $E_{pa}$ ) and cathodic peak potential ( $E_{pc}$ ). A redox couple in which both species rapidly exchange

electrons with the working electrode is termed as electrochemical reversible couple. Such couple can be identified from a cyclic voltammogram by measurement of the potential difference between the two peaks potential. The formal reduction potential  $E^{\circ}$  for reversible couple is centered between  $E_{pa}$  and  $E_{pc}$  (Scholz *et al.*, 2005).

$$E^{\circ} = \frac{E_{pa} + E_{pc}}{2} \quad (1)$$

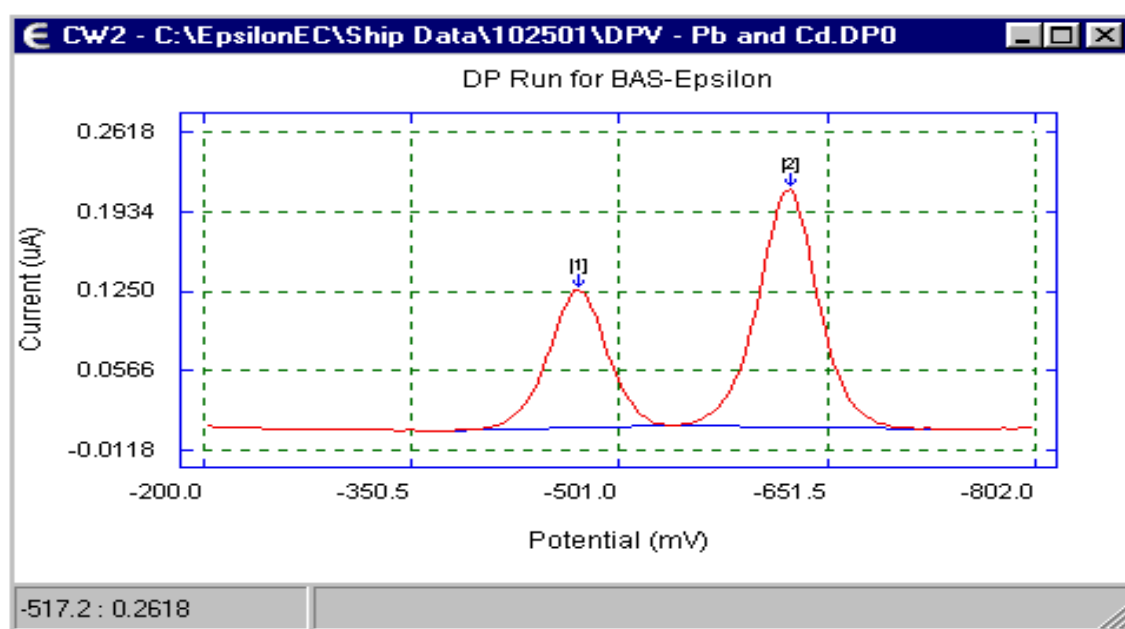
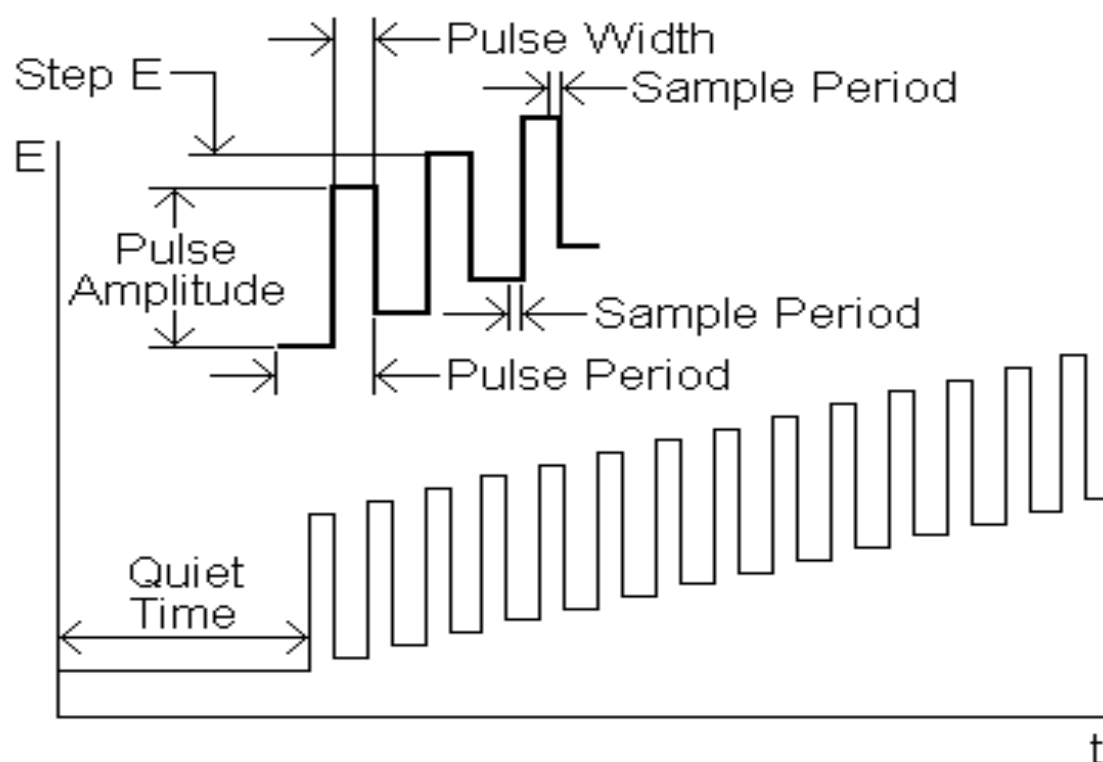
The number (n) of electrons transferred in the electrode reaction for reversible couple can be determined from separation between peak potentials.

$$\Delta E = E_{pa} - E_{pc} \quad (2)$$

### 2.9.2. Differential Pulse Voltammetry

This technique is comparable to normal pulse voltammetry in that the potential is also scanned with a series of pulses. The basis of all pulse techniques is the difference in the rate of the decay of the charging and the faradaic currents following a potential step (or "pulse"). However, DPV differs from NPV because each potential pulse is fixed, of small amplitude (10 to 100 mV) and is superimposed on a slowly changing base potential. Current is measured at two points for each pulse, the first point just before the application of the pulse and the second at the end of the pulse. These sampling points are selected to allow for the decay of the nonfaradaic (charging) current.

The difference between current measurements at these points for each pulse is determined and plotted against the base potential. Consider a reduction ( $Ox + e \rightleftharpoons Red$ ), at potentials well positive of the redox potential, there is no faradaic reaction in response to the pulse, so the difference current is zero. At potential around the redox potential, the difference current reaches a maximum, and decreases to zero as the current becomes diffusion controlled. The current response is therefore asymmetric peak Figure 5 (Kissinger *et al.*, 1996).



b)

Figure 5. a) Excitation wave form of differential pulse Voltammetry. b) DPV response

### 3. MATERIALS AND METHODS

In this chapter the synthesis and characterization for the nanocomposites are presented. The construction of ZnO, extended graphite sheet (EGS), extended Graphite sheet/ZnO nanocomposites electrochemical sensor on glass carbon electrode (GCE) and its electrochemical characterizations are outlined.

#### 3.1. Experimental Site

The synthesis of extended graphite sheet, ZnO NPS, extended graphite sheet/ZnO nanocomposite, Uv-Vis characterization of the synthesized nanocomposites and electrochemical detection of para-nitrophenol, CV and DPV electrochemical characterization of the modified electrodes were conducted in the Chemistry Department Laboratory of Haramaya University. X-ray diffraction (XRD) and Fourier transform infrared spectroscopy (FTIR) characterization were done in Addis Ababa Science and Technology University Department of Chemistry Laboratory.

#### 3.2. Instruments and Apparatus

The instruments that were used in the study include; XRD (BRUKER D8 Advanced XRD, Germany), Spectrum 65 FTIR, Uv Vis spectrophotometer (SANYO, SP65, GALAN AKAMP, made in U.K), centrifuge, oven, electrical furnace (analytical balance (OHAUS, made in Switzerland), deionizer, polishing pad, beaker, ceramic crucible, volumetric flask, pipettes, mortar, sonicator, magnetic stirrer, test tubes, cuvette (quartz), beakers and pH meter (MP220). The electrochemical analyzer (Bas100B) with three electrode configurations was used throughout the experiments with a modified GCE as working electrode, a platinum wire as auxiliary/counter electrode. All the cell potentials were measured with respect to an Ag/AgCl [KCl (sat)] reference electrode.

### 3.3. Reagents and Chemicals

The chemicals that were used during the synthesis of the nanocomposite include sulphuric acid (MW: 98.08 g/mol, 98% from Mumbai), nitric acid (MW: 63.03 g/mol, 69% from Mumbai), ethanol (99.7%, absolute grade from MERCK and ALDRICHE), zinc nitrate hexahydrate (98%, reagent grade from SHANGHAI), alumina powders (0.05  $\mu\text{m}$ ) (were purchased from Böchler), Sodium carbonate (99%, from ALDRICH), hydrochloric acid (37%), para nitrophenol, potassium chloride, potassium ferri hexacyanide ( $\text{K}_3\text{Fe}(\text{CN})_6$ ),  $\text{NaH}_2\text{PO}_4 \cdot 2\text{H}_2\text{O}$ ,  $\text{Na}_2\text{HPO}_4$ , sodium hydroxide, graphite flake and ammonia. All the chemicals are analytical grade and were used without further purification and all solutions were made up with distilled and double deionized water.

### 3.4. Experimental Procedures for the Synthesis of Nanocomposites

#### 3.4.1. Synthesis of Extended Graphite Sheet

Extended graphite sheet was prepared by a chemical reduction method. A mixture of concentrated sulfuric acid 240 mL and 60 mL nitric acid (4:1V/V) was mixed with 4g graphite powder at room temperature and stirred continuously for 16 h. The acid-treated natural graphite was then washed thoroughly with water until the solution become neutral and was dried at 100 °C to remove the remaining moisture. The dried particles were heated at 1050 °C for 15 seconds to obtain reduced graphite particles. The reduced graphite was then immersed in a 70% of aqueous alcohol solution and was treated to powdering in ultrasonic bath (ultrasonicator) for 8 h. The resulting dispersion was then filtered and dried to get extended graphite nano sheets (Rajesh *et al.*, 2012).

#### 3.4.2. Synthesis of ZnO Nanoparticle

Zinc oxide nanoparticles were prepared by a precipitation method (Bashami *et al.*, 2015). Two solutions were prepared: Solution A (0.1 M of  $[\text{Zn}(\text{NO}_3)_2 \cdot 6\text{H}_2\text{O}]$ ) was prepared by dissolving 5.95g of Zinc nitrate hexahydrate  $[\text{Zn}(\text{NO}_3)_2 \cdot 6\text{H}_2\text{O}]$  in 200 mL distilled and demonized water; and solution B (0.1 M  $\text{Na}_2\text{CO}_3$ ) was prepared by dissolving 2.12 g of

sodium carbonate in 200 mL distilled and deionized water. After that, the precursor was prepared by adding solution A to solution B drop wise under vigorous stirring for 2 h. The precipitate resulting from the reaction between the two solutions was allowed settling down for 24 h, and then filtered with 0.2  $\mu\text{m}$  membrane filter (Whatman) and washing three times each with DI water and ethanol. The precipitate was dry at 100 °C for 6 hr to form the precursor for ZnO. The precursor obtained after drying was calcined at 300 °C for 24 h in programmable furnace to get the nano-ZnO particles (Chen *et al.*, 2008).

### **3.4.3. Synthesis of Extended Graphite Sheet/ZnO Nanocomposite**

The preparation of extended graphite sheets/ZnO (EGS/ZnO) nanocomposite was carried out in ultrasonic spray pyrolysis using chemical reduction. In a typical procedure, 0.85 g of graphite sheet was first dispersed in 50 mL of DI water by sonication for 4 min. Then, the graphite sheet suspension was added with stirring to 2.5 g of Zinc nitrate hexahydrate [ $\text{Zn}(\text{NO}_3)_2 \cdot 6\text{H}_2\text{O}$ ] dissolved in 50 mL of DI water subsequently and sonicated for 6 h to form homogeneous mixing. After 30 min, 0.52 mL of aqueous  $\text{NH}_3$  solution of 0.3 M was added drop by drop. The mixture was heated to 180 °C and maintained at that temperature for 5 h. The color of the resulting extended graphite sheet/ZnO powder was then changed into grayish white. The product was subjected to repeated washing with ethanol followed by centrifugation, and finally washing with water. The pure extended Graphite sheet/ZnO powder was obtained after drying the product over at 60 °C for 1 h (Mathialagan *et al.*, 2017).

### **3.4.4. Preparation of Buffer Solution**

0.1 M phosphate buffers were prepared by weighing 0.8 g of  $\text{NaH}_2\text{PO}_4 \cdot 2\text{H}_2\text{O}$  and 6.518 g of  $\text{Na}_2\text{HPO}_4$  then dissolving in to a 500 mL volumetric flask. It was adjusted with 0.1 M HCl or 0.1 M NaOH to the desired pH (5 to 8) and the final volume was made up to the mark volume with deionized water. All buffer solutions were stored in a refrigerator at 4 °C.

### 3.5. Structural Characterization of the As-Synthesized NPs

#### 3.5.1. X-ray Diffraction

X-ray Diffraction (XRD) measures the average spacing between layers or rows of atoms, the orientation of a single crystal or grain, the crystal structure of an unknown material, the size, shape and internal stress of small crystalline regions. The powder X-ray diffraction patterns of the as-synthesized nanocomposites were obtained using a BRUKER D8 Advance XRD, AXS GMBH, Karlsruhe, West Germany X-ray diffractometer (XRD) equipped with a Cu target for generating a Cu K $\alpha$  radiation (wavelength 1.5406 Å). The measurements were made at room temperature and the accelerating voltage and the applied current were 40 kV and 30 mA, respectively. And the instrument was operated under step scan type with step time and degree (2 $\theta$ ). The identification of a species from its powder diffraction pattern is based upon the position of the lines (in terms of 2 $\theta$ ) and their relative intensities (Chen *et al.*, 2011). The average crystallite size of the as-synthesized nanocomposite can be calculated using the Debye-Scherrer equation (Lv *et al.*, 2011).

$$D = 0.9\lambda / \beta \cos\theta \quad (3)$$

Where D is the average crystallite size,  $\lambda$  is the wavelength of the X-ray = 0.15406 nm for Cu target K $\alpha$  radiation,  $\beta$  is the full width of half-maximum (FWHM) in radian, and  $\theta$  is the Bragg diffraction angle.

#### 3.5.2. Fourier Transform Infrared Spectroscopy

FTIR spectroscopy (Fourier Transform Infrared Spectroscopy) is a technique that uses infrared light to observe properties of the synthesized solid. It is used in many different applications to measure the absorption and emission of radiation by shining a narrow beam of infrared light at the matter in various wavelengths and detecting how the matter responds to each wavelength. Therefore, the as-synthesized nanocomposites were characterized using FTIR (Spectrum 65 FTIR (PERKINELMER) in the range of 4000-400 cm<sup>-1</sup> to assign functional groups, instruments and measurements were performed with

pressed pellets (KBr) made using Paraffin as diluents. About 5 to 10 mg of sample was placed onto the surface face of a KBr plate, a small drop of paraffin was added and the second window was placed on the top (Stuart, 2004).

### **3.5.3. UV-Vis Absorption Measurement**

For the estimation of the absorption edge electronic properties of the as-synthesized nanomaterials, Uv-Vis diffuse absorption was measured. It measures the intensity of light passing through a sample using SP65 spectrophotometer scanning over 200-800 nm and uv-vis absorption spectra of pure ZnO nanoparticle, extended graphite sheet and extended graphite/ZnO nanocomposite were measured in hydrochloric acid solvent.

## **3.6. Electrochemical Measurements**

### **3. 6.1. Preparation of Modified Glass Carbon Electrode**

The bare glassy carbon electrode (GCE) was polished with alumina slurry of 0.05  $\mu\text{m}$  on polishing pad until it forms a mirror-like surface, then rinsed with distilled water to remove the remaining particles from the electrode surface. Then a solution of 4 $\mu\text{L}$  EGS, ZnO and EGS/ZnO nanocomposite was prepared by dissolving 2mg in 2mL ethanol and casted on the surface of bare glassy carbon electrode by drop coating. The modified electrode was then rinsed with distilled water subsequently; the modified electrode was stabilized in 0.1 M PBS by scanning the potential between  $-0.5\text{V}$  and  $+1.2\text{ V}$  until a steady cyclic voltammogram was obtained. Finally, the modified electrode was dried in air and made ready for use. These processes were done before every experiment. Cyclic voltammetric (CV) experiments were performed with 100Bas electrochemical bioanalyzer, All experiments were carried out with a conventional three-electrode system, with a platinum wire as counterelectrode, Ag/AgCl/Cl<sup>-</sup> as reference electrode, and a bare glassy carbon electrode and glassy carbon electrode after modification with EGS, ZnO and EGS/ZnO composite were used as the working electrode. All experiments were carried out at the room temperature.

### 3. 6.2. Electrochemical Determination of Para-Nitrophenol

Chemical sensors are generally estimated by measuring current response at a fixed potential after addition of the analyte for chemical sensing applications and it is a more sensitive method when compared to other methods. The electrochemical detection of p-NP was studied on bare EGS/ZnO and EGS/ZnO modified electrode in 0.1M PBS using DPV and CV from -0.5 V to + 1.2 V at the scan rate of 50mV/s.

### 3.6.3. Optimization of the Sensor

To determine the optimum pH for the electrode, the pH of the reaction buffer was tested from pH 5.0 to 8.0, each at a final concentration of 0.1 M PBS. To study the effect of substrate concentration, different p-nitrophenol concentrations, ranging from 0.001 to 2M were used. For the interference study, the salts of metal ions, namely Zn(II), Cd(II) and Pb(II) were added into the reaction mixture (each at final concentration of 0.1 M), the current response of the sensor was measured both before and after addition of the standard solution.

### 3.6.4. Analytical Performance of EGS/ZnO/GCE

The stability, limit of detection, limit of quantification and reproducibility of the resulted sensor was investigated in this work. The long-term stability of the developed sensor was investigated by measuring its current response to p-nitrophenol over 10 days under ambient conditions, where  $I_0$  is the current response of fresh sensor and  $I$  is the current response after storage. The current of fresh sensor and storage sensor was compared. The reproducibility of successive DPV measurements for five different 0.1M p-nitrophenol carried out with the same sensor was checked by calculating the relative standard deviation of the steady current (Kumar *et al.*, 2013; Wang *et al.*, 2012). The limit of detection (LOD) and limit of quantification (LOQ) of the DPV for p-nitrophenol sensor was estimated using the formula in Equations (4).

$$\text{LOD} = 3S_b/m \quad (4)$$

Where  $S_b$  is the standard deviation obtained from the measurements of the signal and  $m$  is the slope value that was extracted from the calibration plot and the sensitivity value was also estimated from the calibration.

### **3.6.5. Real Sample Analysis**

The proposed method was applied for the determination p-nitrophenol in industrial waste water. 100mL waste water, sample was collected from Drie leather industry in Addis Ababa. The sample was then filtered by 0.2  $\mu$ M Whatman filter paper. The practical application of the proposed sensor (extended graphite sheet/ZnO/GCE) was evaluated by testing the p-nitrophenol concentration in the sample. DPV studies were performed before and after addition of p-nitrophenol into the samples using the extended graphite sheet/ZnO/GCE modified electrode at an applied potential. From calibration curve concentrations were extrapolated and recovery was calculated by dividing the obtained concentration to the spiked one.

## 4. RESULTS AND DISCUSSION

### 4.1. Structural Characterization of the Nanocomposites

#### 4.1.1. X-ray Diffraction

The characteristic XRD patterns of the as synthesized EGS, ZnO and EGS/ZnO nanocomposites are shown in Figure 6. The diffraction peaks at scattering angles ( $2\theta$ ) around 31.02, 32.65, 34.45, 36.50, 42.8, 47.7, 50.80, 56.7, 60.76, 63,66.5, 68.04 and 69.2 ° suggesting the wurtzite crystalline structure of ZnO (Chen *et al.*, 2011). Major peak of EGS are formed at an angle ( $2\theta$ ) of 19.24, 26.02, 28.92, 30.6, 32.5, 33.42, 36.04, 57.8 and 63.38° and other small peaks also appeared that indicates the orthorhombic crystalline structure of EGS and indicate the properties of carbon in EGS. The peak appearing at 19.2, 26.02 and 28.9° is due to the presence of oxygen carrying groups on the EGS surface which was significantly decreased in EGS/ZnO nanocomposite (Figure 6c) due to exfoliation of EGS as a result of the ZnO NCs surface loading.

Figure 6c illustrates that the XRD patterns of the as-synthesized nanocomposite EGS/ZnO. The characteristic of small peaks in EGS have broadened and these peaks are still in accordance with the zincite phase of ZnO, which indicating the incorporation of the nanocomposites is more intensive and implying a good crystalline nature of the as-synthesized ZnO product. On the other hand, the EGS/ZnO nanocomposite also exhibits the similar planes corresponding to the ZnO wurtzite structure. In addition to the ZnO diffraction peaks, the appearance of a weak broad peak is attributed to the characteristic peak of EGS. Therefore, EGS/ZnO nanocomposite is highly remarkable which indicating the formation of well crystalline structure of ZnO NCs onto the EGS surface.

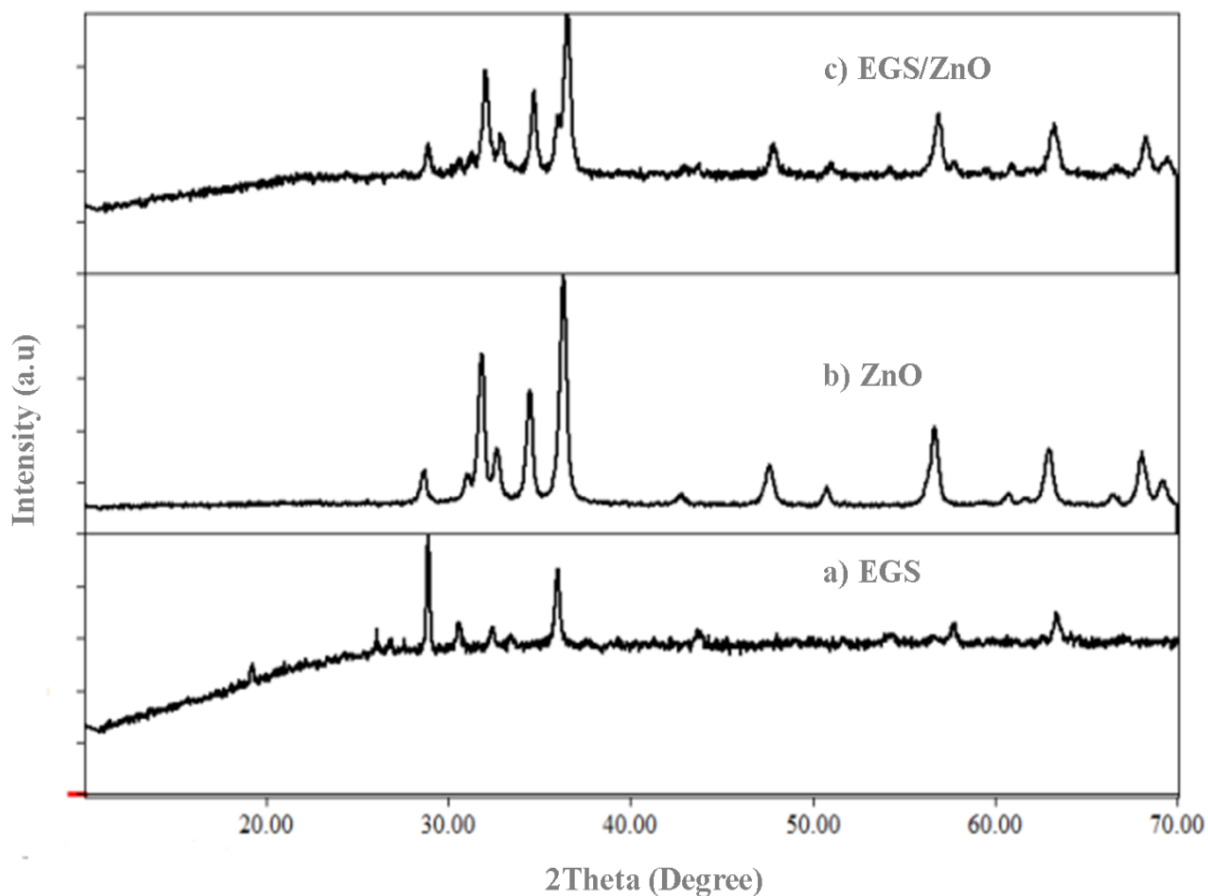


Figure 6. XRD spectra of EGS, ZnO and EGS/ZnO nanocomposites

The crystalline size of each nanocomposite was calculated from the main diffraction peaks by using Scherer formula (equation 3) is indicated in the Table 3. The Order of average crystallite size ( $D$ ) of as-synthesized nanocomposites are  $\text{EGS/ZnO} < \text{ZnO} < \text{EGS}$  which indicates a good formation of the nanostructure.

Table 3. Average crystallite size ( $D$ ) of as-synthesized Nanocomposites

Sample	$2\theta$ (Degree)	$\beta$ (Radian)	$D$ (nm)
EGS	28.91	0.00279	51.35 nm
ZnO	36.4	0.008378	17.55 nm
EGS/ZnO	36.71	0.012566	11.625 nm

#### 4.1.2. Fourier Transform Infrared Spectroscopy Analysis

The FTIR spectra of EGS, ZnO and EGS/ZnO nanocomposite (Figure 7) shows a broad band around  $\sim 3431\text{cm}^{-1}$  corresponding to stretching mode of OH group which may be due to the vibration mode of OH group of water (Ahmed *et al.*, 2011). This indicates that the existence of small amount of water absorbed by the nanocomposite and it shows an increase in the transmittance from EGS, ZnO and EGS/ZnO respectively due to the increase in the surface area of the nanocomposites and the peak around ( $1720\text{--}1740\text{ cm}^{-1}$ ) indicates C=O Stretching vibration. The peak at 1626 is the bending vibratio of HOH in water. Comparing the spectra of EGS/ZnO nanocomposite with that of EGS demonstrates a slight shift with a reduction in the intensity of the O–H peak ( $3431\text{ cm}^{-1}$ ). Besides, the peak at about  $1740\text{ cm}^{-1}$  corresponding to C=O was disappeared in EGS/ZnO nanocomposite. This confirms the formation of ZnO NCs onto the surface of EGS accompanied by a partial reduction of the EGS.

The strong and sharp peak at  $\sim 1375\text{cm}^{-1}$  may be attributed to the bond of carbon-oxygen-zinc and also a strong and sharp peak at about  $662\text{ cm}^{-1}$  may be due to the bond between EGS with metalzincoxide nanoparticles. Small peaks appeared around  $\sim 600$  and  $\sim 611\text{ cm}^{-1}$  are due to O-C-O stretching vibrations of the monodentate carbonate species. The peak appearing between  $\sim 411$  and  $551\text{ cm}^{-1}$  is assigned to the metal - oxygen (M–O) stretching modes (Sharma *et al.*, 2011). This demonstrates that the EGS are incorporated on the surface of ZnO nanoparticles.

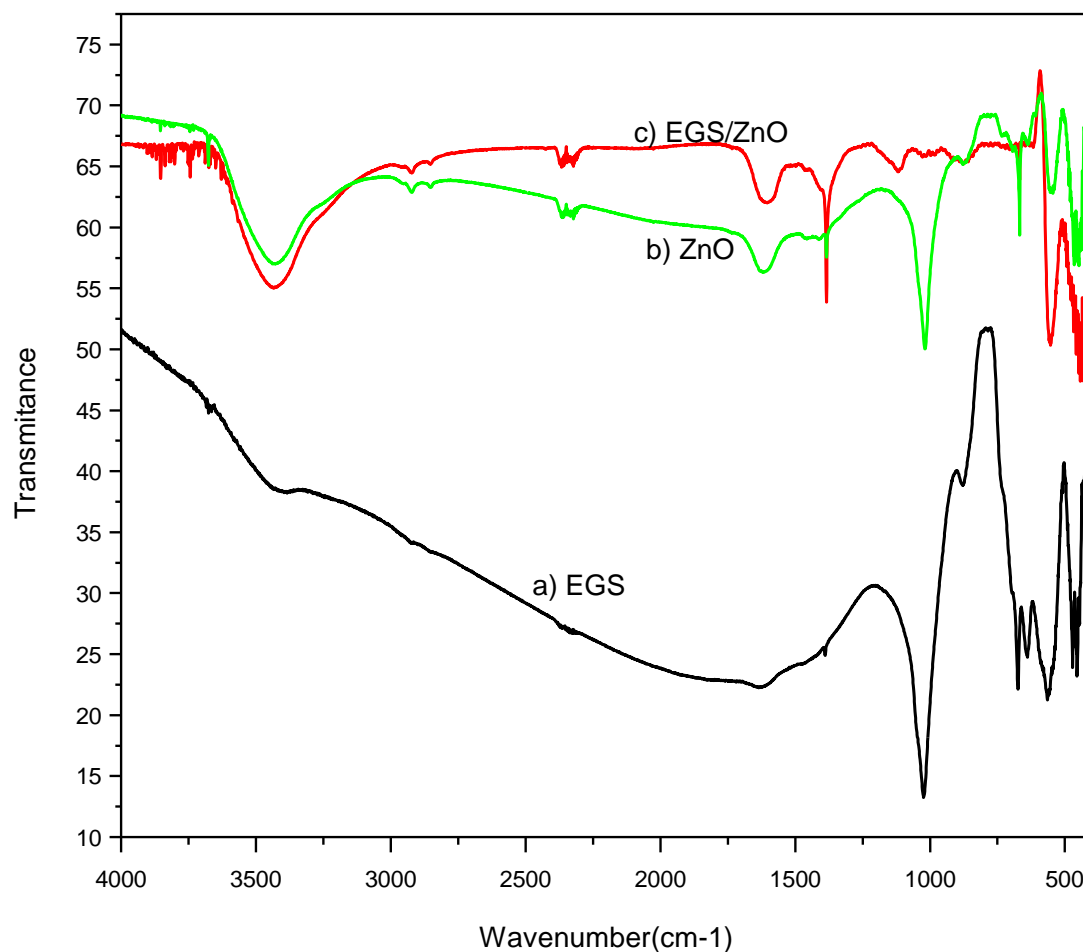


Figure 7. FTIR Spectra of a) EGS, b) ZnO and c) EGS/ZnO nanocomposites.

#### 4.1.3. UV- Visible Analysis

UV-Vis absorption spectra of the synthesized EGS, ZnO, EGS/ZnO nanocomposite is shown in Figure 8. Their corresponding absorption maxima are: 320, 385, and 460 nm, respectively. It can be seen that ZnO nanoparticles showed strong absorption band in the UV region than EGS. In the case of EGS/ZnO nanocomposite, the absorbance has increased in the entire region and the absorption edge is shifted towards higher wavelength region due to the incorporation of graphite sheet. The bandgap energy of graphite sheet incorporated ZnO is lower (2.71 eV) than bare ZnO (3.22 eV). Therefore, this result indicates the narrowing of the band gap of ZnO with the addition of EGS. The reduction in

bandgap of ZnO with the addition of graphite sheet might be attributed to the chemical interaction between ZnO and extended graphite sheet. This may be due to creation of localized energy levels by EGS in the band gap of ZnO. The optical absorption edges of the EGS/ZnO obviously shifted further to the visible region compared to ZnO and EGS and a significant enhancement of the visible-light absorption is obvious. Thus the improvement of the visible-light absorption can be attributed to the graphite sheet nanotubes sensitizing for zinc oxide nanoparticles due to their larger surface area and the presence of metallic zinc contributes the narrowing of band gap of ZnO nanocomposite. The bandgap energy  $E_g$  of the as-synthesized nanocomposite was obtained using the relation (El- Kemaary *et al.*, 2010).

$$E_g \text{ (eV)} = 1240/\lambda \quad (5)$$

Where,  $E_g$  is band gap energy in electron volts and  $\lambda$  is wavelength (nm) corresponding to absorption maxima. The  $E_g$  of the nanocomposite EGS, ZnO, and EGS/ZnO were found as 3.87, 3.22 and 2.71 respectively Table 4.

Table 4. Absorbance and maximum wavelengths of the as-synthesized nanoparticles

Sample	Max.wavelength(nm)	Band gap ( $E_g$ ) (eV)
EGS	320	3.87
ZnO	385	3.22
EGS/ZnO	460	2.71

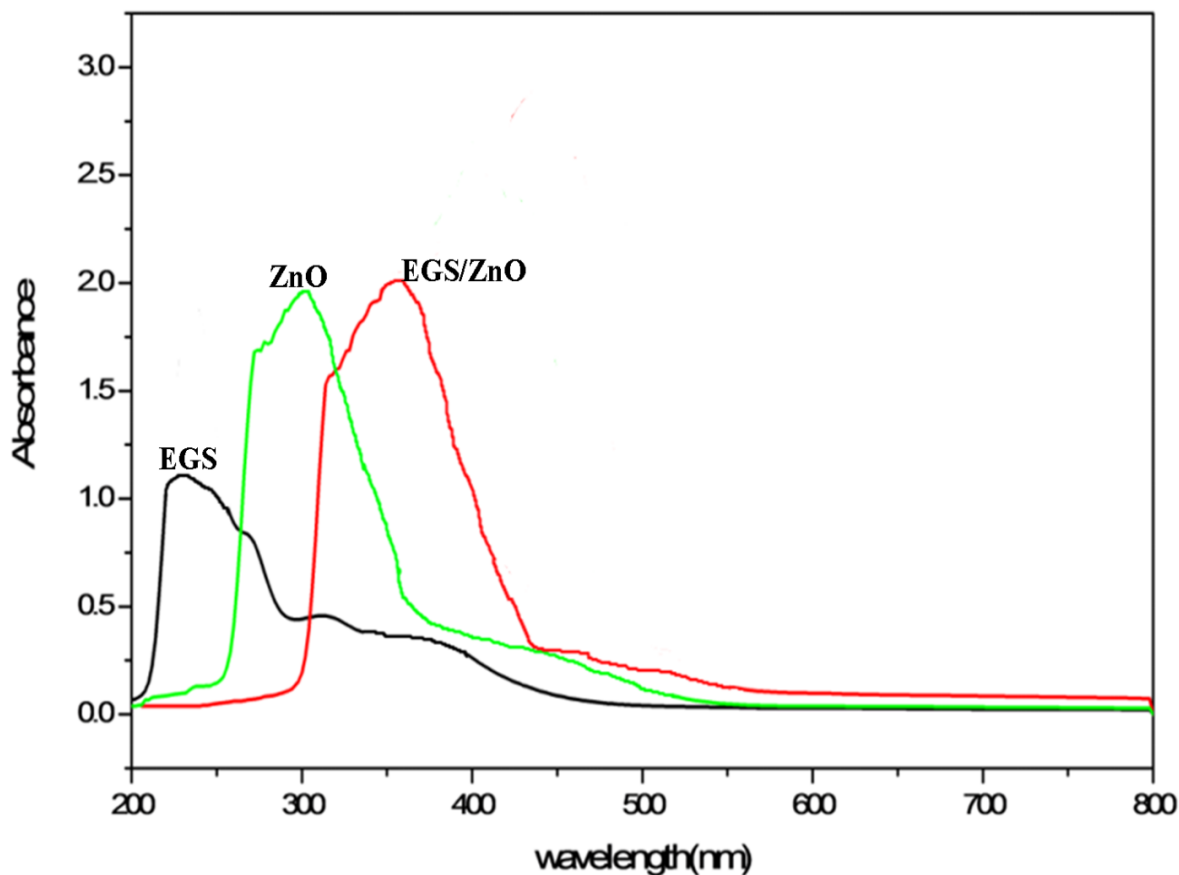


Figure 8. Uv-visible absorption spectra of EGS, ZnO and EGS/ZnO nanocomposites

## 4.2. Electrochemical Characterization of the Nanocomposites

### 4.2.1. Electrochemical Characterization of the Various Modified Electrodes in Potassium Ferro Cyanide

Potassium ferrocyanides was used as a redox probe by studying the voltammetric behavior of the unmodified GCE due to its sensitivity to surface chemistry and microstructure. The cyclic voltammogram of GCE in 2 mM  $\text{K}_3\text{Fe}(\text{CN})_6 + 0.1\text{M}$  KCl at potential range from  $-0.5$  to  $+1.2\text{V}$  and at different scan rates is shown Figure 9 and its various electrochemical parameters are evaluated and summarized in Appendix Table 1. The effects of scan rate on peak potential of the other parameters was examined at different scan rates from 10 to 100 mV/s.

The cyclic voltammetry curves recorded displays one oxidation and reduction peak. As the scan rate increases the anodic and cathodic peaks potentials approximately/nearly constant and also the difference in anodic and cathodic peaks potentials is in the range 148 to 240 mV, which confirms that the reversibility of the process (Roa *et al.*, 2003; Beltagi *et al.*, 2011) but  $I_{pa}$  and  $I_{pc}$  of the cyclic voltamogram increases as the scan rate increase. The difference redox potential of  $K_3Fe(CN)_6$  at scan rate of 50 mV/s was found 90 mV in agreement with the reported value (Zhang *et al.*, 2000). Detail electrochemical parameters of  $K_3Fe(CN)_6$  on GC electrode are evaluated and indicated in appendix Table 1.

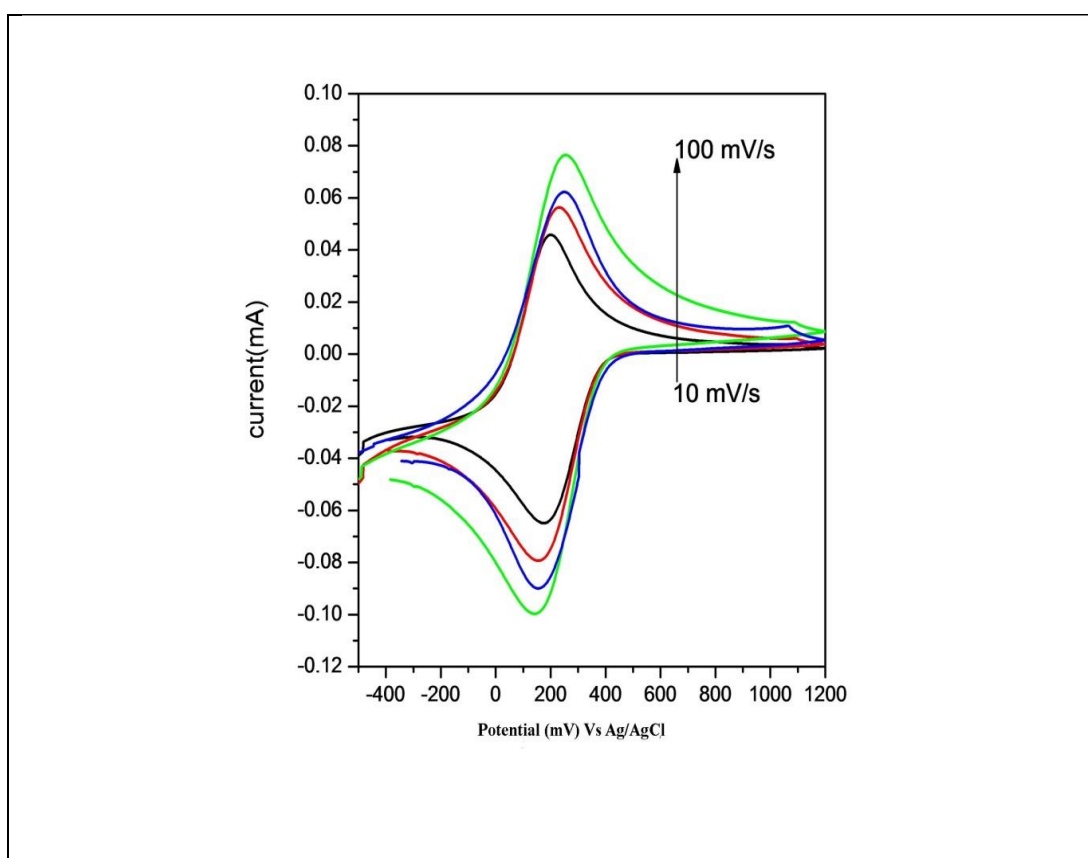


Figure 9. CV of GCE in  $K_3Fe(CN)_6$  at different scan rate ranging from 10 to 100 mV/s.

The oxidation or the reduction peaks shows a slight increased after incorporating the nanomaterials especially at high scan rates, either EGS, ZnO or EGS/ZnO, in to the electrode matrix as shown in Appendix Table 2. As the scan rate increases the oxidation peak potential shifts to more positive value which is a typically characteristics of movement of ions in and out of films. In the case of the of EGS/ZnO nanocomposite the

peak current enhanced due to the catalytic properties of graphite sheet and the conjugation of EGS to the ZnO nanoparticles enhanced the electron transfer or this may be probability of EGS amount in the composite and highly incorporation of ZnO nanoparticle in the electrode which may create a good catalytic activity to free movement of ions and EGS role in the composite could be demonstrated as a wire-transfer for bridging the electron between the ZnO (that accepts the electrons from the redox molecules) and the electrode surface.

Figure 10 Shows the typical cyclic voltammetry (CV) of bare GCE and modified GCE in the 0.1 M KCl solution containing 2mM  $K_3Fe(CN)_6$ , which is sensitive to the surface chemistry of carbon based electrodes. The reduction and oxidation peak current increased obviously after the modified GCE, and the redox peaks current of EGS/ZnO/GCE became even higher than the others (EGS and ZnO) at the scan rate of 50mV/s. The oxidation peak current of bare GCE was around 0.055 mA (a), EGS/GCE 0.076 mA (b), ZnO/GCE 0.085 mA (c), GS/ZnO/GCE 0.098 mA and the peak-to-peak separation ( $\Delta E_p$ ) at bare GCE, EGS/GCE, ZnO/GCE and EGS/ZnO/GCE was 75, 69, 35 and 52 mV respectively as shown Appendix Table 2. The oxidation peak current increased obviously and the  $\Delta E_p$  decreased correspondingly, indicating the presence of EGS/ZnO/GCE can fast the electron transfer.

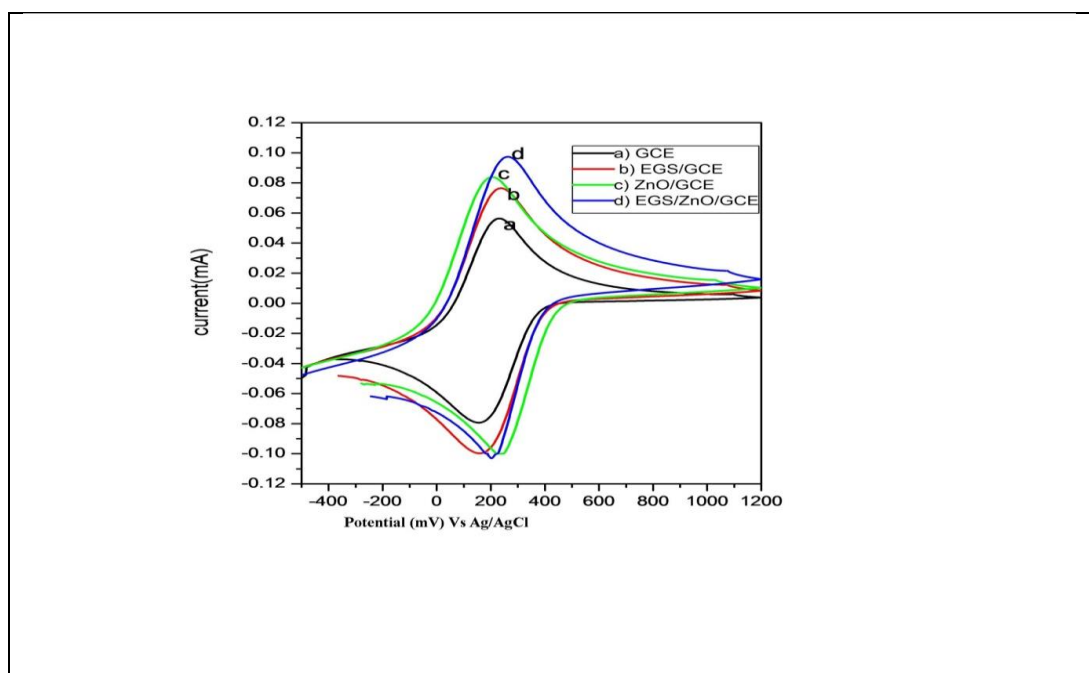


Figure 10. Cyclic voltammograms of a) GCE b) EGS/GCE c) ZnO/GCE d) EGS/ZnO/GCE

#### 4.2.2. Electrochemical Characterization of the Modified Electrode in 0.1M PBS

The CV results of the EGS/GCE, ZnO/GCE and EGS/ZnO/GCE in 0.1 M phosphate buffer solution (pH 6.5) at different scan rates (10 to 100 mV/s) are shown in Figure 11. Cyclic voltammograms recorded in the course of the nanocomposites in 0.1M PBS aqueous solution on bare and modified GC electrode in a potential range -0.5 to 1.2 V and at scan rate of 50mV/s are shown in Appendix Table 3. The origin of the anodic waves is attributed to the oxidation of the nanocomposites to its radical anion and the anodic waves are as a result of the oxidation of the nanocomposites deposited at the electrode surface which oxidation occurs at the electrolyte PBS. The oxidation and reduction peak is increasing in the EGS/ZnO/GCE nanocomposite which shows good electron transfer.

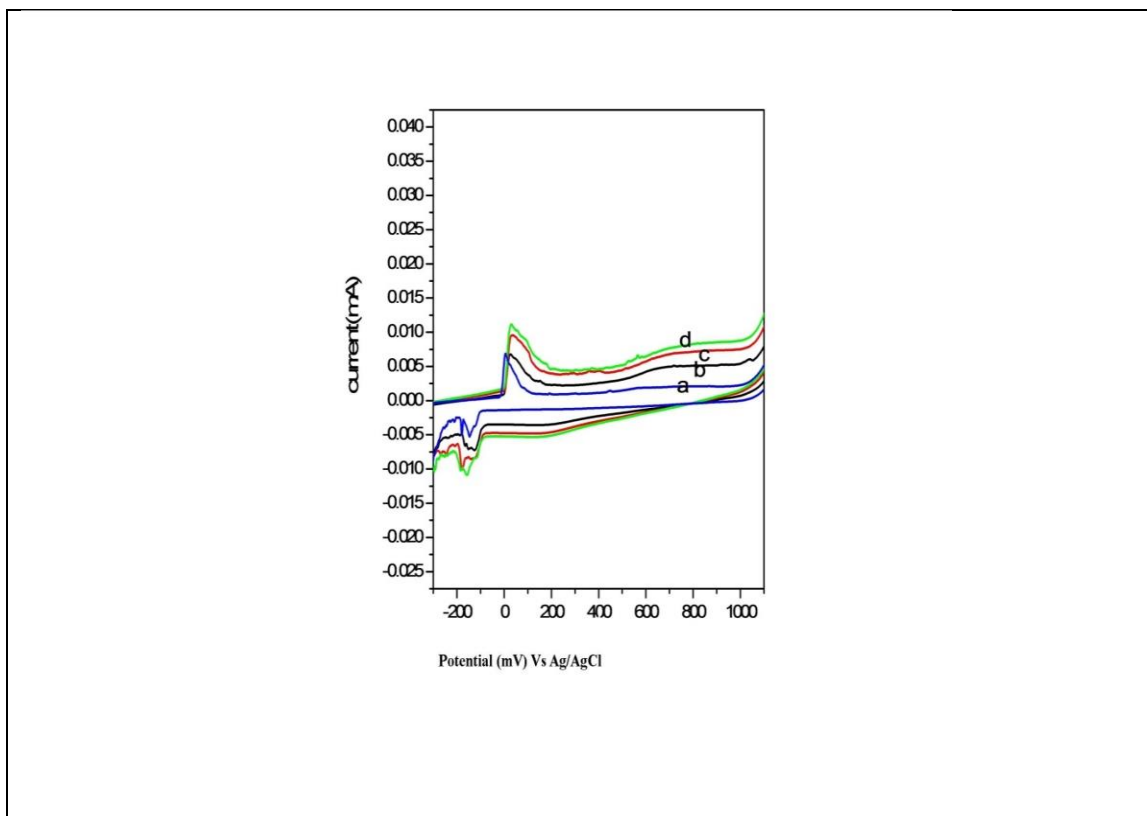


Figure 11. Cyclic voltammograms of a) GCE b) EGS/GCE c) ZnO/GCE d) EGS/ZnO/GCE

### 4.2. 3. Electrochemical Impedance Spectroscopy

The analysis was performed in the frequency range from 0.1Hz to 1000Hz by applying Dc EIS potential of 193 mV and voltage of AC amplitude 5mV. Figure12 Shows the EIS of the EGS/GCE, ZnO/GCE and EGS/ZnO/GCE recorded in 0.1M PBS (pH=6.5). The diameter of the semicircle in the high frequency region corresponds to the charge transfer resistance for EGS/GCE is 223.9 $\Omega$  in contrast the charge transfer resistance value of ZnO/GCE decreased to 221.6 $\Omega$  which shows the ZnO/GCE facilitates the electron transfer process. After compositing EGS with ZnO the charge transfer resistance value further decreased to 200.5 $\Omega$  which indicating the low interfacial electron transfer resistance and good electron transfer properties. So the binary system facilitates the electro-oxidation of p-nitrophenol due to the high capacity surface area of EGS and catalytic properties of the two nanocomposites.

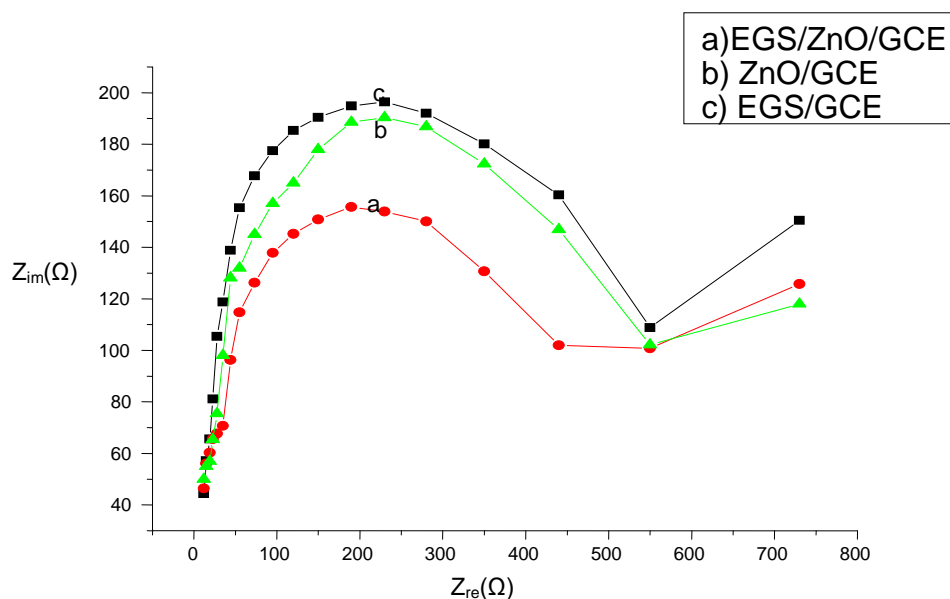


Figure 12. Impedance curve of the different modified electrodes in 0.1M of PBS

#### 4.2.4. Cyclic Voltammetry Behavior of the Sensor in p-Nitrophenol

To evaluate the catalytic activity of EGS/ZnO/GCE, the modified electrode was characterized using a cyclic voltammogram in the potential range from  $-0.2$  to  $+1.1$  V. Figure 13 Shows cyclic voltammograms of the EGS/ZnO/GC electrode in a solution containing 0.1M phosphate buffer +KCl, (pH 6.5) without p-Np (curve a) or with 0.1M p-Np (curve b) at a scan rate of 50 mV/s. A particular redox peak was observed for the EGS/ZnO/GC electrode in phosphate buffer (curve a) with  $E_{Pa}$  27mV and  $I_{Pa}$  0.007mA as well as reduction peak current with  $E_{Pc}$  -113 mV and  $I_{Pc}$  0.0074mA. When p-Np was added into phosphate buffer, however, the CV of the EGS/ZnO/GC electrode shows a peak potential of  $E_{Pa}$ =296 mV,  $E_{Pc}$ = 62 mV,  $I_{Pa}$ =0.009mA and  $I_{Pc}$ =0.011mA (curve b). Apparently, this peak comes from the oxidation of p-nitrophenol which is catalyzed by the immobilized EGS/ZnO/GCE.

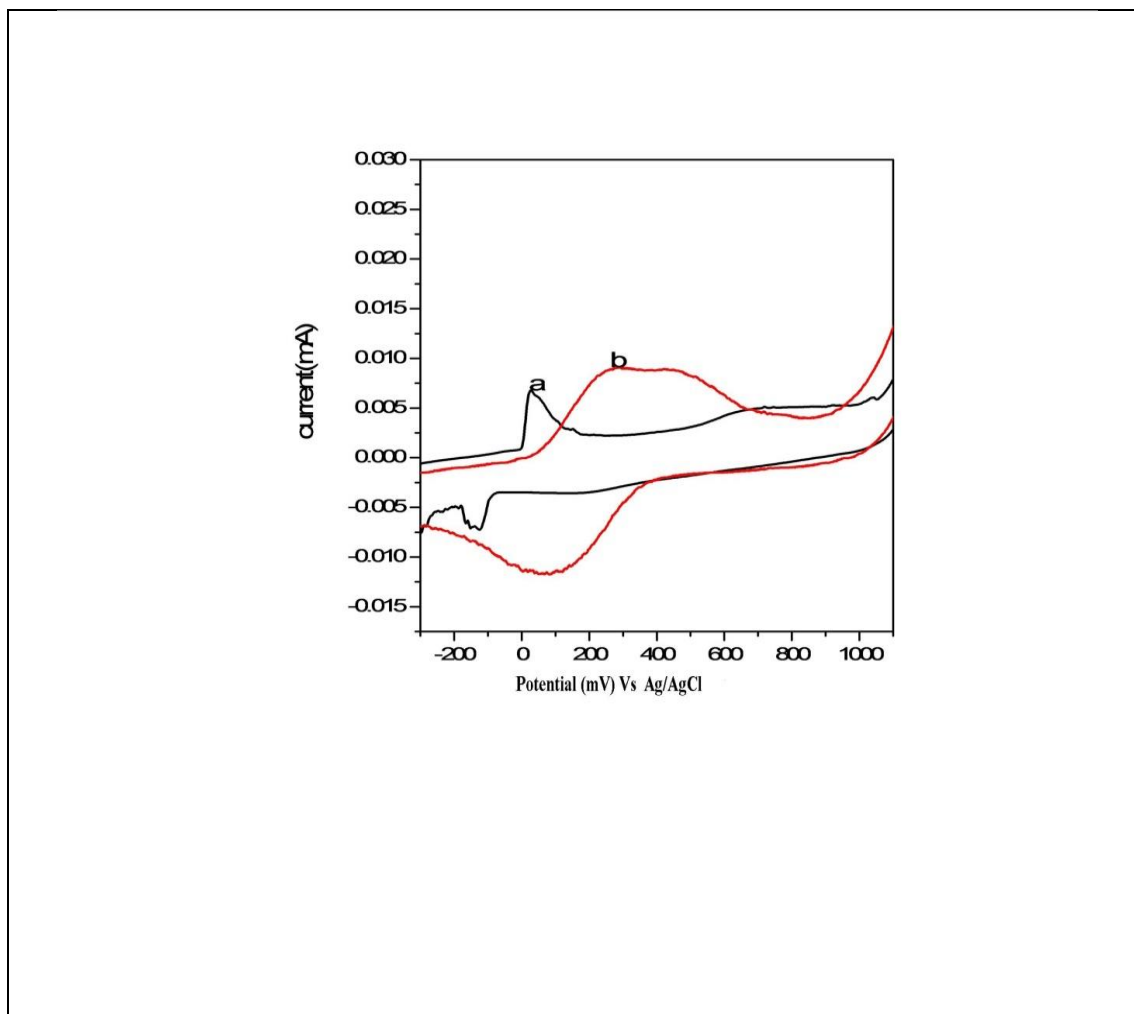


Figure 13. Cyclic voltammogram of the EGS/ZnO/GCE electrode in 0.1M PBS (pH 6.5) in the absence (a) and presence (b) of 0.1M p-NP.

As the main concern of this study it is enable to the direct detection of p-NP using the developed nano-structured electrode, the capability of direct electron transfer was tested. In this regards, 0.1M concentrations of p-NP was injected in to the electrochemical cell and the direct oxidation of the nanocompositewas measured. In order to investigate the oxidation and reduction behavior of p-Np and the effect of scan rate of the oxidative and reductive peak current on EGS/ZnO/GCE in 0.1 M phosphate buffer solution (pH 6.5) and potential range of -0.5V to 1.1V were investigated. Figure 14 demonstrates that both the oxidative and reductive peak current of p-Np increased with scan rate (10 to 100 mV/s). The potentials ( $E_{pa}$  and  $E_{pc}$ ) shifts toward more negative for  $E_{pc}$  and shifts

towards more positive for  $E_{pa}$ , indicating that both potentials ( $E_{pa}$ ,  $E_{pc}$ ) are functions of scan rates and sensitivity also increases.

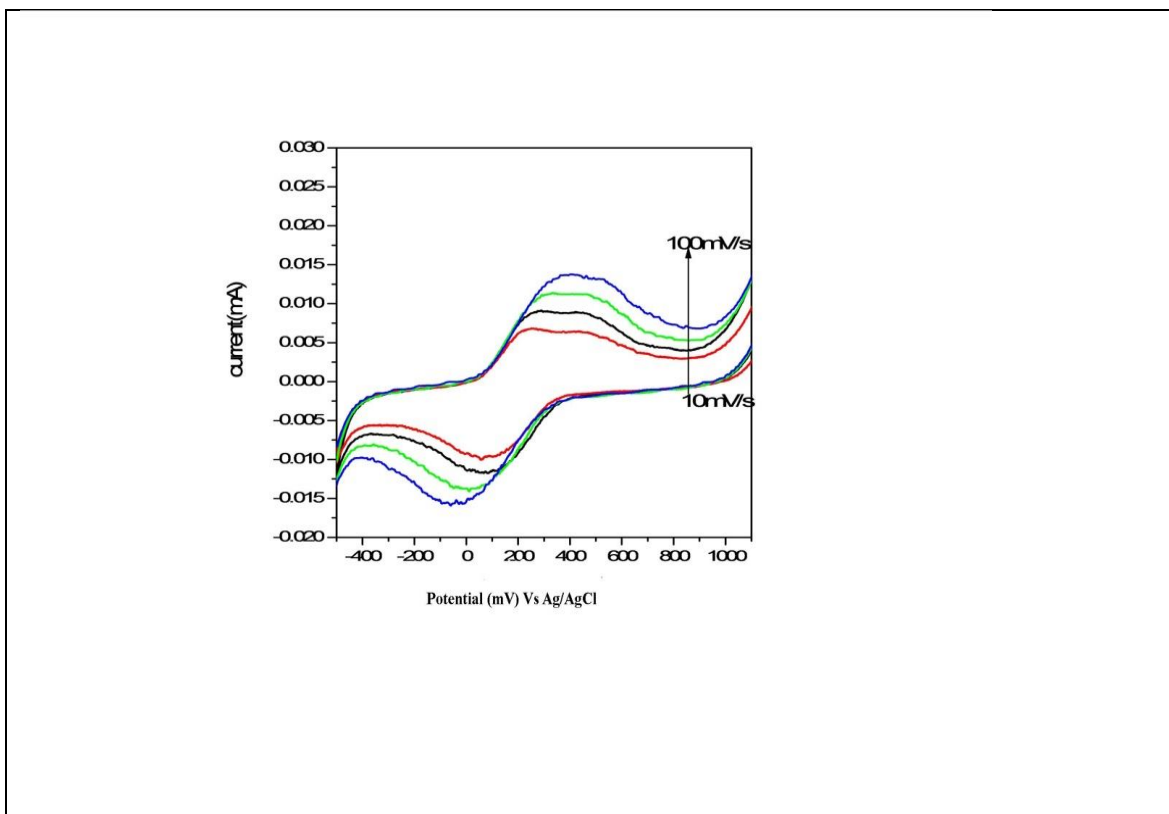


Figure 14. Cyclic voltammograms of EGS/ZnO/GCE in 0.1M of PBS (pH 6.5) and 0.1M p-Np.

To evaluate the catalytic activity of GCE, EGS/GCE, ZnO/GCE and EGS/ZnO/GCE electrode, the modified electrode was characterized using a cyclic voltammogram in the presence of 0.1M of p-nitrophenol in the potential range from  $-0.5$  to  $+1.1$  V at the scan rate of  $50\text{mV/s}$ . The cyclic voltametric responses of the nanocomposite were much higher than that obtained by either the ZnO-based electrode EGS or bare GCE. Therefore, the used nanostructured electrode has then enough electro catalytic activity to enable the direct detections of p-nitrophenol. In addition, the oxidation currents were correlated with the concentrations of p-Np and that reflects the sensitivity as well as the reliability of the proposed sensor. The changes of current with 0.1M p-NP on various modified ZnO/GCE, EGS/GCE, EGS/ZnO/GCE and unmodified electrodes are presented in Figure 15. A

significant enhancement of current is achieved with EGS/ZnO/GCE composites for p-NP owing to the high surface area of EGS and high electro active property of ZnO in composites material (Low *et al.*,2016). Better absorption and adsorption capacity onto the porous graphite sheet and ZnO hybrid surfaces.

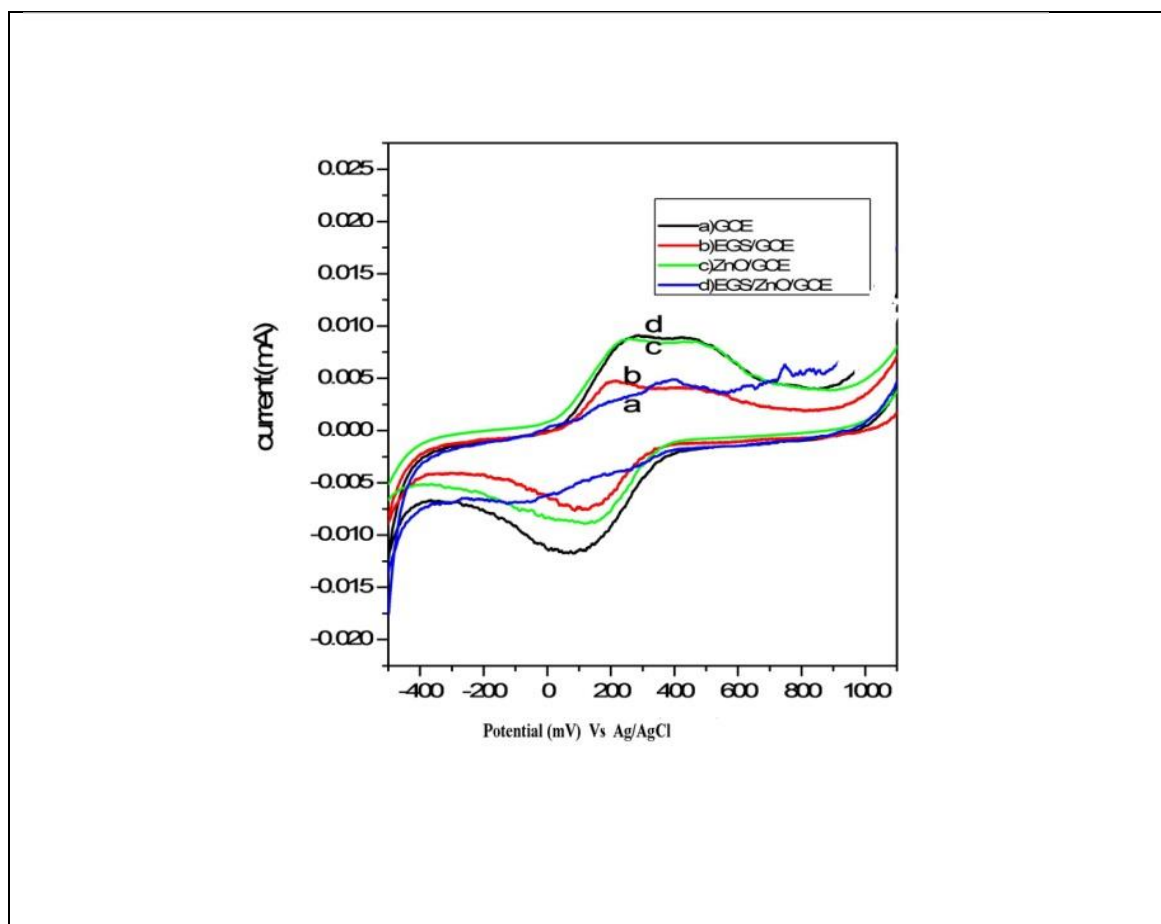


Figure15. Cyclic voltammograms on a) GCE b) EGS/GCE c) ZnO/GCE d) EGS/ZnO/GCE of 0.1M p-NP in 0.1M PBS at scan rates of 50mV/s.

### 4.3. Optimization of the EGS/ZnO/GCElectrode

#### 4.3.1. Effect of pH

The solution pH affects the performance of the electrochemical response of the electrodes. The relationship between pH of the solution and peak current in 0.1M p-NP is shown in

(Figure16). The peak current increased with the increasing PH from 5.0 to 6.5. Further increasing the pH of the buffer solution caused the peak current to decrease. Furthermore, within the pH range of 5.0 to 6.5, the oxidation reduction peak potential increased gradually, whereas from 7.0 to 8.0 it decreased gradually, indicating low electron transfer rate (Harrison *et al.*, 1993).

The pH value of the solution has a significant influence on the peak current and peak potential of catalytic oxidation and reduction of p-Np (Figure 16) shows that at higher pH, current was decreased due to hydroxylation of the mediator. Moreover, potential shifted to more negative due to proton involved in electrochemical reaction of p-NP. On the other hand at lower pH current decreased due to common ion effect (Figure 17). This indicates that peak current of p-NP reaches maximum value at (pH 6.5). Therefore, pH = 6.5 peak (d) in the (Figure 16) with its calibration curve in (Figure17) shown was taken for further analysis of p-NP on the modified GCE electrode.

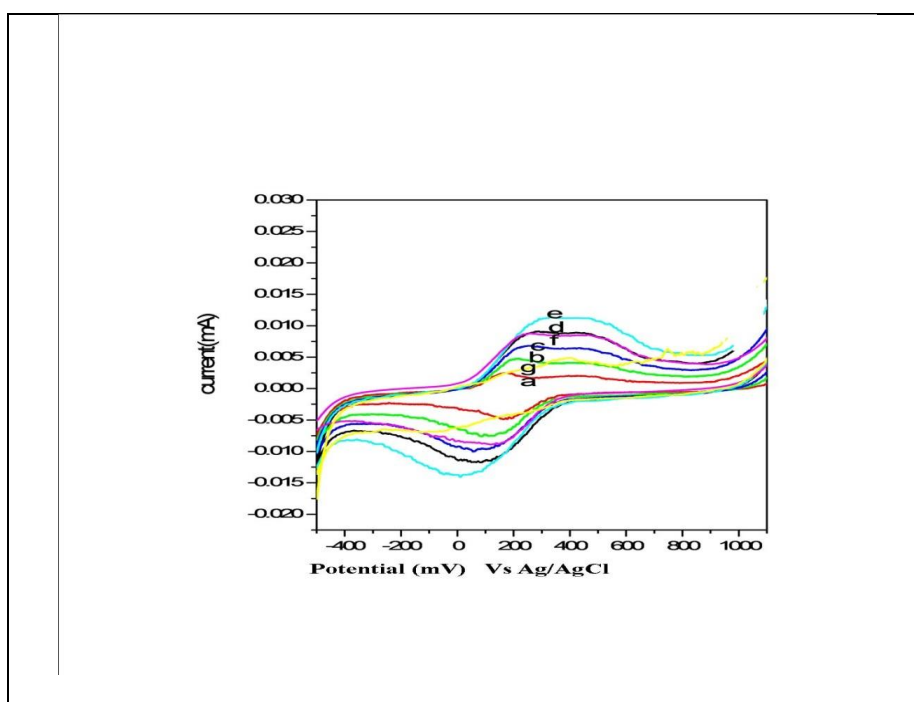


Figure 16. Typical Cyclic voltammograms obtained at EGS/ZnO/GCE in various buffer solutions (pH 5 to 8) at the scan rate of 50 mVs for a solution containing 0.1M p-NP

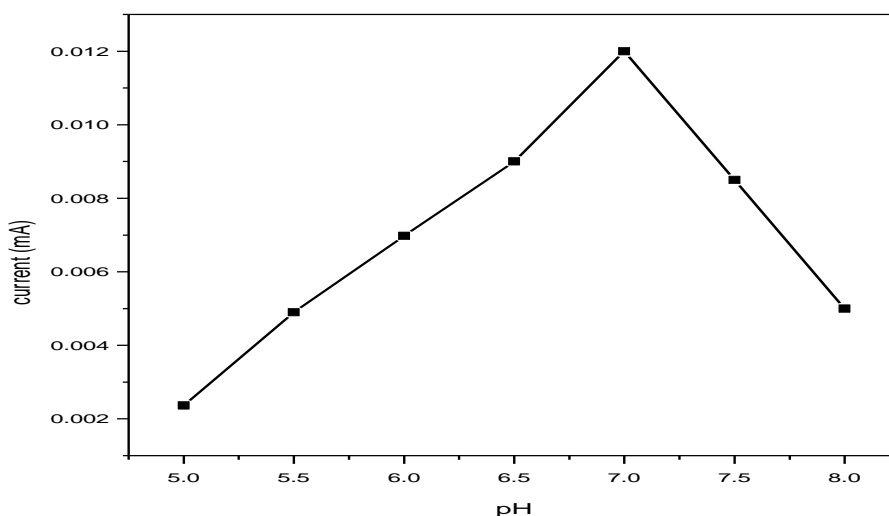


Figure 17. PH versus anodic peak current plot of the CV obtained at EGS/ZnO/GCE in various buffer solutions (PH 5-8) at scan rate of 50mV/s for a solution containing 0.1M p-NP

#### 4.3.2. Effect of Concentration

The effect of concentration was studied by taking 0.001 to 2 M p-NP in 0.1M PBS at (pH 6.5) and scan rate of 50mV/s. There was a linear relationship between the sensor response of EGS/ZnO/GCE and p-NP concentration as shown(Figure 18). Based on these result 2M was selected as the optimum concentration in the subsequent experiments. The calibration curve is plotted by taking various  $I_{pvs}$  concentrations of p-NP (Figure 19). From the calibration curves, it is concluded that the linear dynamic range (0.001–2M), and linearity ( $R^2 = 0.998$ ), have been estimated. The responses of the EGS/ZnO/GCE that were examined with different concentration (0.001–2M) of p-NP, shows the changes of current of the fabricated electrode as function of p-NP concentration under room conditions. It is observed that the current responses are amplified usually from lower to high concentration of the target analyte. A good range of the analyte concentrations (0.01 to 2M) has been examined from the low to high potential (-0.5 to 1.1 V) to observe of the possible analytical parameters.

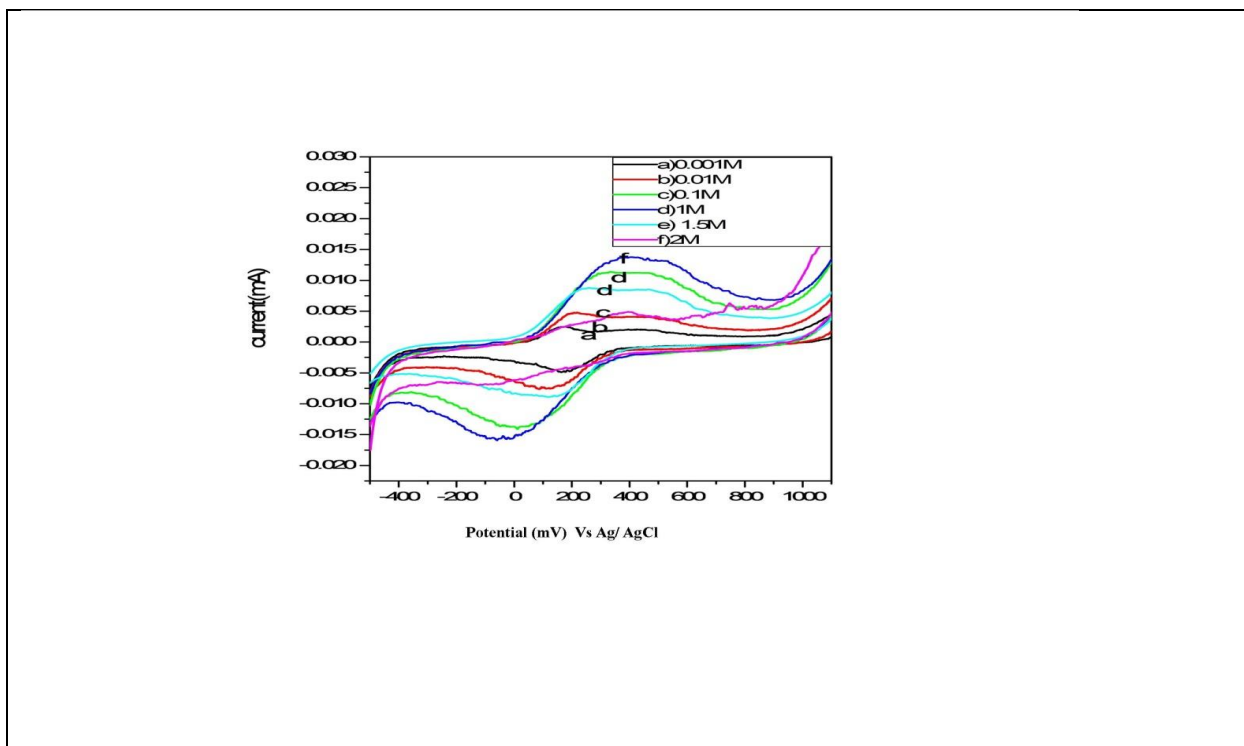


Figure 18. Cyclic voltammograms of EGS/ZnO/GCE at different concentrations p-Np.

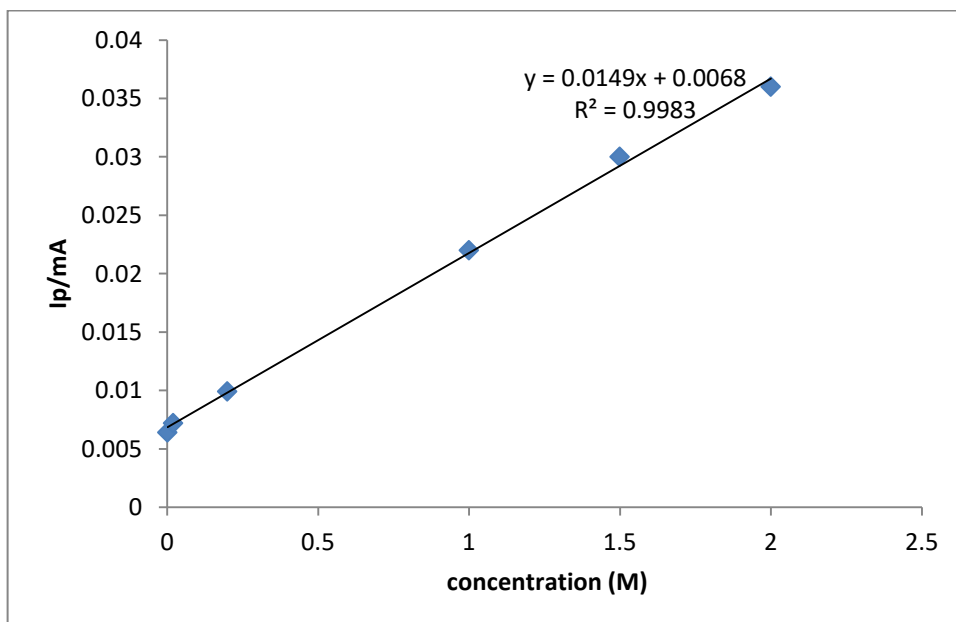


Figure 19. Calibration plot for current versus concentrations of p-NP

### 4.3.3. Effect of Interference

Heavy metal ions can inhibit the activity of EGS/ZnO/GCE and hinder p-Nitrophenol detection. The addition of 0.1M of heavy metals like zinc, cadmium and lead salts at the applied potential (-0.5 to 1.1V and scan rate of 50 mV/s as can be seen in (Figure 20), the peak to peak separation of the analytes were very small as a result, there is a determination of one analyte in the presence of the metal ions because their oxidation and reduction potentials are close resulted and the activity decreases of only 2.6% for Zn(II), 3.9% for Cd(II), and 2.6% for Pb(II) as shown in figure 20. Therefore, heavy metal ions have practically no effect on the sensor response for the detection of p-Nitrophenol.

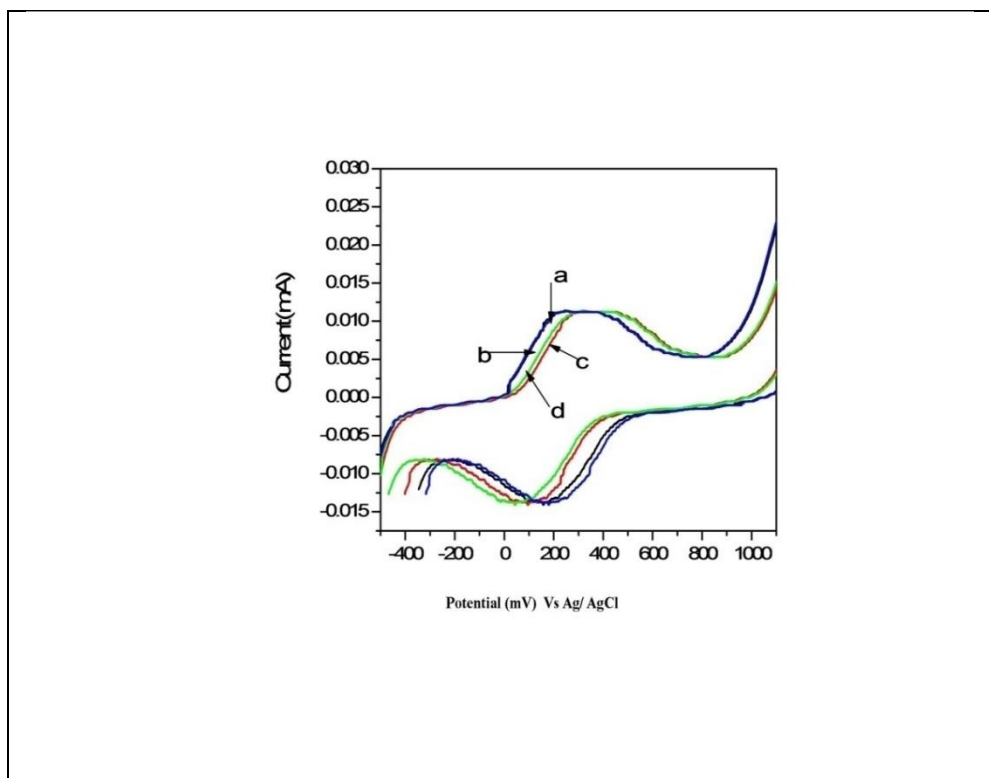


Figure 20. Cyclic voltammograms of EGS/ZnO/GCE with (a) no heavy metals, (b) lead metal (c) cadmium and (d) zinc metal concentration in 0.1 M of p-Nitrophenol

#### 4.4. Electrochemical Detection of p-Np under Optimized Parameters

The high sensitivity of the developed oxidation peak ( $E_{pa}=234\text{mV}$ ) at the GCE modified with EGS/ZnO/GCE at 0.1M PBS (pH 6.5), suggests possible application of the developed DPV method for analysis of para-nitrophenol. Figure 21 shows that the DPV curves for the standard solution of p-NP on the EGS/ZnO modified GCE over the concentration range of 0.001-2M and 0.1M PBS (pH 6.5). It can be clearly observed that the potential of peak current for electrochemical detection is at about 284mV and the inset in Figure 22 shows the linear relationship between the peak currents and the concentrations from 0.001 to 2M with the linear  $I (\mu\text{A}) = 0.016C (\mu\text{M}) + 0.002$  ( $R^2=0.999$ ), where C stands for the concentration of p-NP. The limit of detection (LOD) and the limit of quantification (LOQ) were calculated using the following equations:  $\text{LOD}=3\text{SB}/b$ ,  $\text{LOQ}=10\text{SB}/b$ , where SB is the standard deviation of the y-intercepts and b is the slope of the calibration curve. So the LOD and LOQ are  $0.00234\mu\text{M}$  and  $0.0234\mu\text{M}$  respectively. From calibration plot the sensitivity of modified electrode was determined by using the slope of calibration plot ( $a=0.014\mu\text{A}\mu\text{M}^{-1}\text{cm}^{-2}$ ) and the standard deviation ( $\alpha$ ) was 0.0109 (Figure 22). The high sensitivity of the developed oxidation peak ( $E_{pa}=284\text{mV}$ ) at the GCE modified electrode with at pH 6.5 suggests possible application of the developed DPV method for analysis of p-NP. Under the optimum experimental conditions is pH 6.5, pulse amplitude 5 mV, pulse width 50 ms with frequency range of 0.1-1000Hz and potential range of (-0.5 to 0.8V). Therefore DPV shows that the peak current increased linearly with increasing the p-NP concentration in the range from 0.001 to 2M by DPV method.

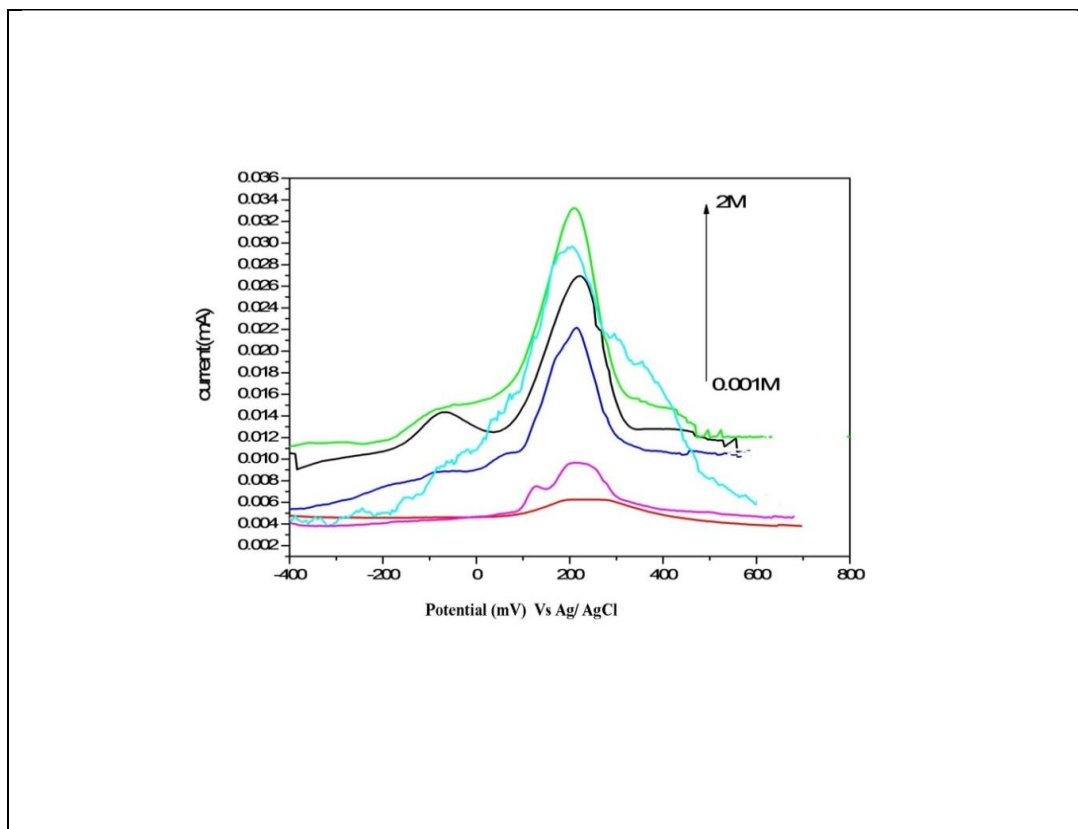


Figure 21. DPV voltammogram of standard solutions of p-NP (0.001- 2M) at pH 6.5, pulse amplitude 5 mV, pulse width 50 ms and scan rate 50 mV/ s

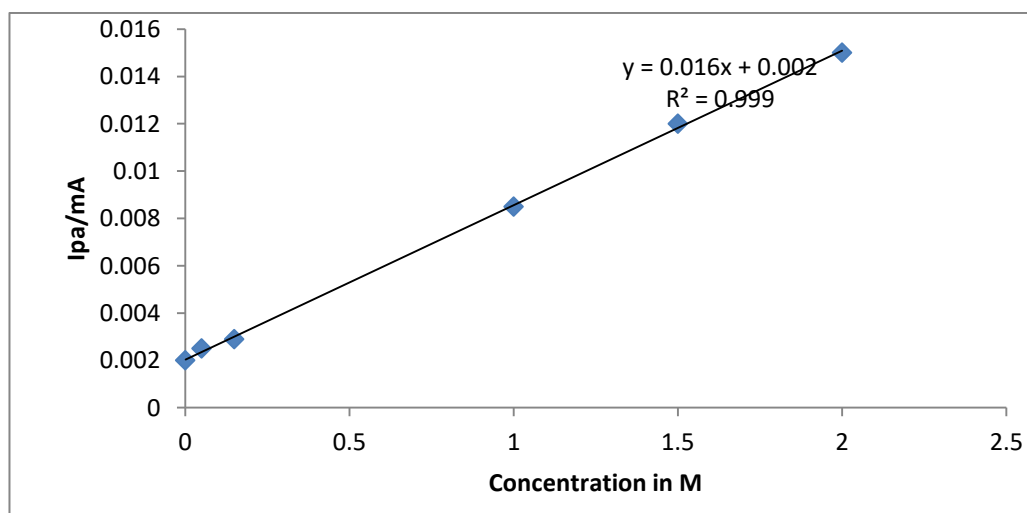


Figure 22. Calibration plot of current versus concentrations of p-NP

#### **4.4.1. Reproducibility and Stability Test**

To estimate the repeatability of the proposed method, the RSD of five successive measurements of peak current of 2M p-NP on single modified electrode was calculated to be 3.8% which demonstrates that good reproducibility of the method. In order to determine stability of the EGS/ZnO/GCE for p-NP detection performance of the electrode was monitored every two days for consecutive 10 days by analyzing their relationship between the peak current and storage days. During 10 days storage period, the EGS/ZnO/GCE NPs electrode retained 97% of initial response current which revealing good storage stability.

#### **4.5. Determination of p-Nitrophenol in Waste Water using EGS/ZnO/GCE**

In this study, while optimizing all parameters, DPV was run for the solution containing only the supporting electrolyte. The industrial waste water sample that was used in this work did not contain detectable amount of p-nitro phenol, hence the sample was spiked with 2M concentration of p-nitrophenol solution. From the calibration curves plotted for the known standard solution of p-nitrophenol, the unknown concentration of p-nitrophenol (value of X) was successfully calculated by using equation  $y = mX + b$  obtained from the calibration curves of the standard solution. In this case the value of "b" is intercept and m (slope) and the value of y (peak current) was obtained from the DPV (Figure 22) recorded for p-nitrophenol in waste water sample. In such extracted sample, recovery experiment was performed and the experiment done in triplicate. The calculated amount of p-NP concentration in waste water sample was determined. These results are presented in Table 5. Which shows that recovery values around 99.0% was found for the waste water sample as shown in Figure 23 .

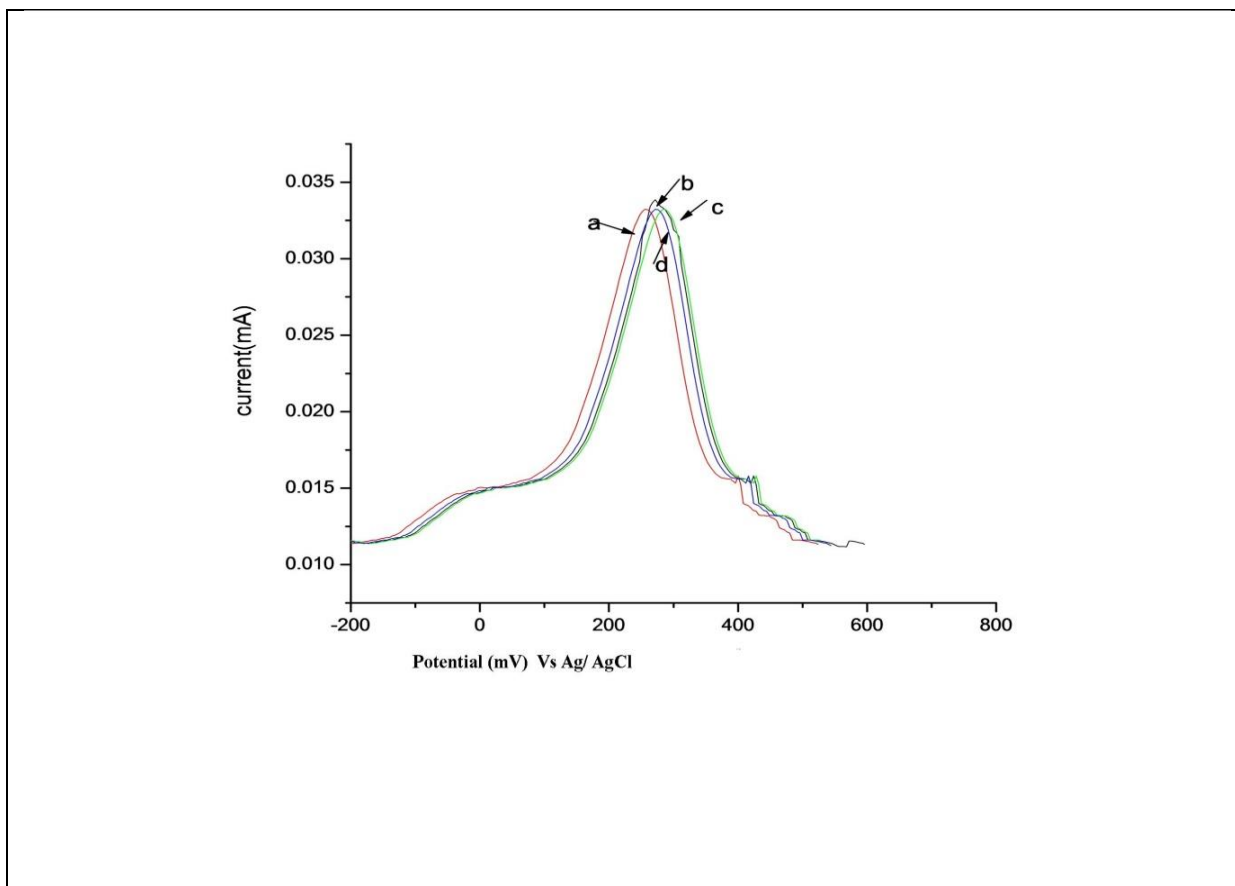


Figure 23. DPV of 2 M p-Nitrophenol concentration in industrial waste water sample a) standardized solution b, c and d up on addition standard solution to the sample

#### 4.5.1. Recovery Test

Recovery of the experiment was performed to examine the potential applications of the EGS/ZnO/GCE. So EGS/ZnO/GCE sensor was adopted to detect the concentration of p-NP in industrial waste water and before detection the pH of waste water was adjusted to 6.5 with 0.1M PBS. Therefore, as the results listed in Table 5. The average recovery of three independent experiments for p-NP were calculated to be 99% .These results indicates that the method was better for analysis p-NP in industrial waste water.

Table 5. Detection of p-NP from the waste water sample

Real sample	Added	Found	Recovery
7ml	3ml of 2M	1.93	96.5%
7ml	2M	2.007	100.4%
7ml	2M	1.993	99.7%
Average	2M	1.98	99%

## 5. SUMMARY, CONCLUSIONS and RECOMMENDATIONS

### 5.1. Summary and Conclusion

Extended Graphite sheet, ZnO, and EGS/ZnO nanocomposites are produced using chemical reduction and precipitation method. The synthesized nanocomposites were characterized by using UV-visible, FTIR, XRD techniques. The chemically produced EGS, ZnO and EGS/ZnO modified electrodes were characterized by cyclic voltammetry and EIS in 2mM  $K_3Fe(CN)_6$  aqueous solution and 0.1M PBS solution. The cyclic voltammetry shows that the deposited EGS/ZnO on GCE was more electro active due to the high surface area of EGS. In addition to this the EIS spectra shows low charge transfer resistance value in comparison to the other which indicating fast electron transfer.

The developed EGS/ZnO/GCE sensor was optimized with pH of 0.1M phosphate buffer solution from pH of 5 to 8. The peak current was recorded in pH solution of 6.5. When optimized conditions, the EGS/ZnO/GCE sensor was used to determine p-Np in standard solution 0.001 to 2 M using CV and DPV. The electrode exhibits a linear range of 0.01 to 2 M, sensitivity of 0.014, limit of detection 0.00234  $\mu$ M, limit of quantification 0.0234  $\mu$ M and with linearity ( $R^2=0.998$ ). Besides the sensor also applied to detect p-Np in industrial waste water. The concentration of p-Np was not detected by the sensor, therefore, spiking 3 mL of 2 M p-Np to 7 mL of sample was carried out. Furthermore, the performance of the sensor shows with good stability, reproducibility. Effect of interference also studied using Zn, Pb and Cd salt solutions, the current was decreased only 2.6% for Zn(II), 3.9% for Cd(II), and 2.6% for Pb(II). Therefore, the developed p-NP sensor's response practically not affected by heavy metal ions. So the developed EGS/ZnO sensor was highly selective and sensitive under the optimum conditions with linear range concentration 0.01–2 M and high recovery values around 99%. Therefore, EGS/ZnO/GCE sensor can be a potential candidate for the detection of p-Np.

## 5.2. Recommendations

- Further research should be carried out to explore the effect of composition of ZnO, EGS, EGS/ZnO of the nanocomposite.
- Optimization to understand the electrode deposition time, temperature, methods of synthesis, surface electrode and studying other interference should be taken into account.
- The electro catalytic activity of the as-synthesized nanocomposite should be done by modifying the electrodes with Conducting binding agents (like 5% nafion).
- Synthesizing the nanomaterials in various methods of synthesizing method of nanoparticles.

## 6. REFERENCES

- Ahmed, F., Shalendr,K., Nishat,A., Anwar,M.S., Lee,S.Y., Gyung Suk,K., DaeWon,P., Bard, H.K., Faulkner, A.J, andL.R..2001.Electrochemical Methods: Fundamental and Applications. *2nd edition, John Wiley*, New York, 244 - 246.
- Bashami, R., M.A., Hameed, M., Aslam, Iqbal, M.I., Ismail, M.and, Tahir, S. 2015.The suitability of ZnO film-coated glassy carbon electrode for the sensitive detection of 4-nitrophenol in aqueous medium. *Analytical Methods*, 7: 1794-1801.
- Bon, G.L.Chan. 2011. Preparation and characterizations of polyaniline (PANI)/ZnO nanocomposites film using solution casting method. *Thin Solid Films*, 519 : 8375–8378.
- Busca, G., Berardinelli, S., Ressini, C. and Arrighi, L. 2008.Technologies for the removal of phenol from fluid streams. *Journal of Hazardous Materials*,160: 265– 288.
- Chao, X.C., Lixin, S., Ge, W., Liu, H., Liu, Y., Yaqin and Xiaofei,Q. 2010. Preparation of ZnO/Cu<sub>2</sub>O compound photo catalyst and application in treating organic dyes. *Journal of Hazardous materials*, 176: 807–813.
- Chen C., Yu,B., Liu,P., Liu, J.F. and Wang,L. 2011. Ceramic Processing Research Investigation of nano-sized ZnO particles fabricated by various synthesis routes. *Journal Ceramic Process*, 12 : 420-425.
- Chu, L., Han, L. and Zhang X.L. 2011. Electrochemical simultaneous determination of nitro phenol isomers at nano-gold modified glass carbon electrode. *Journal of Applied Electrochemistry*, 41: 687-694.
- Chung-Hsiao, Taipei and Taiwan. 2008. Electrochemical sensors and biosensors composed of nanowires. *Journal of Sensing Material*, 8: 290-313.
- Chunhai, Y. 2004. Electrochemical determination of 4-Nitrophenol using a single-wall carbon nanotube film-coated glassy carbon electrode microchim. *Actator*, 148: 87–92.
- Coleman, J. N., Khan,U., Blau,W. J., Y. K and Gunko. 2006. Carbon nano tubes. *A Review*, 44:1624 -1652.

- Crouch, Stanley, Skoog and Douglas, A. 2007. Principles of instrumental analysis, water analysis and determination of organic compounds in natural and treated waters. *London(GBR)Spon Press*, 57: 1039-1041.
- Daniel, S., Rao, T. P., Rao, K. S., Rani, S. U., G. R, K. Naidu, Lee, H. Y., and Kawai, T.. 2007. A review of DNA functionalized/grafted carbon nanotubes and their characterization. *Sensor and Actuators Chemistry*, 122: 672-682.
- Dionex Corporation. 2008. Determination of phenols in drinking and bottled mineral waters using online solid-phase extraction followed by HPLC with UV-Detection. *Phenol for synthesis*, 63: 872-876.
- Dreyer, D.R., S.P., Bielawski, C. Wand Ruoff, R.S. 2010. The chemistry of graphene oxide. *Chemical Society Review*, 39: 228–240.
- Eda, G. and Mansh, C. 2010. Chemically derived graphene oxide towards large-area thin-film electronics and optoelectronics. *Advanced Material*, 22: 2392–2415.
- El Mhammedi, M.A., Achak, M., Bakasse, M. and Chtaini, A. 2009. Electrochemical determination of para-nitrophenol at apatite-modified carbon paste electrode: application in river water samples. *Journal of Hazardous Materials*, 163: 323-328.
- ElKemary, M., ElShamy, H. and ElMehasseb, I. 2010. Photocatalytic degradation of graphene/ZnO nanocomposite for development of enhanced biosensor. *Analytical Chemistry Actator*, 903 : 131–141.
- Gilje, S.H., Wang, M., Wang, K.L and Kaner, R.B. 2007. A Chemical route to graphene for device applications. *Nano Letter*, 7: 3394–3398.
- Guinovart, T., Parrilla, M., Crespo, G.A., Rius, F.X and F.J. 2013. Potentiometric sensors using cotton yarns, carbon nanotubes and polymeric membranes. *Analyst*, 138: 5208-5215.
- Harma, A., Pallavi and Kumar, S. 2011. Synthesis and Characterization of NiO-ZnO nanocomposite sensor for electrochemical detection of para-nitrophenol. *Resource Chemistry Intermediate*, 38: 2443–2455.

- Huang, M.H., Mao, S., Feick, H., Yan, H., Wu, Y., Kind, H., Weber, E., Russo, R. and Yan, P. 2001. Room temperature ultraviolet nanowire. *Nanolasers and Science*, 292: 1897-1899.
- Katwal, R.H., Kaur, G., Sharma, M., Naushad and Pathania, D. 2015. Electrochemical synthesized copper oxide nanoparticles for enhanced photocatalytic and antimicrobial activity. *Journal of Indian Engineering Chemistry*, 31: 173-184.
- Kissinger, P. T.; Heinemann and W. R. 1996. Laboratory techniques in electroanalytical chemistry. *Marcel Dekker, Inc., New York, 2nd edition*, 254 – 255.
- Lete. 2010. New composite materials used in the phenol electroanalysis part I poly (Azulene)/prussian blue and prussian blue/boly (Azulene) films. *Rouan Chemistry*, 55(6): 335-338.
- Lin, K., Pan, J., Chen, Y., Cheng, R and Xu, X. 2009. Study the adsorption of phenol from aqueous solution on hydroxyapatite nanopowders. *Journal of Hazardous Materials*, 161: 231-240.
- Liu, J., Choe, J.K., Sasnow, Z., Werth, C.J and Strathmann, T.J. 2013. Application of a Re-Pd bimetallic catalyst for treatment of perchlorate in waste ion-exchange regenerates brine. *Water Resource*, 47: 91-101.
- Luo, L.Q., Zou, X.L., Ding, Y.P., and Wu, Q.S. 2008. Derivative voltammetric direct simultaneous determination of nitrophenol isomers at a carbon nanotube modified electrode. *Sensors and Actuators*, 135: 61-65.
- Mansor, Bin, Ahmad, Kamyar, Shamel and Majid Darroudi. 2009. Synthesis and Characterization of Nanocomposites by Chemical Reduction Method. *Journal of Applied Sciences*, 6 (11): 1909-1914.
- Megharaj, M., Pearson, H.W., Vekateswarlu and Arch, K. 1991. Toxicity of phenol and three nitrophenols towards growth and metabolic activities of *nostoclinckia* isolated from soil. *Environmental Contamination Toxicology*, 21: 578-585.
- Mohammed, M., Rahmana, A., Asiria, M., Salem, A., Hameed, and Basma, A. 2017. Ultra-sensitive p-nitrophenol sensing performances based on various Ag<sub>2</sub>O conjugated carbon material composites. *Journal of Chemical Sensor*, 8: 73-82.

- Munnik, P., Petra, E. de Jongh, Krijn, Pandde Jong. 2015. *Inorganic Chemistry Review*. 115: 6671-6687.
- Palanisamy, S., Chen, S.M. and Sarawathi, R. 2012. Sensors and Actuators. *Biochemistry*, 255:166-167.
- Parthiban, K., Vignesh, V., Nilmini, V. and Thirumurugan, R. 2015. A statistical approach on optimization of exopolymeric substance production by halomonas and its emulsification activity. *Bioresources and Bioprocessing*, 2: 48-54.
- Rahman, M.M., Jamal, A., Khan, S.B. and Faisal, M. 2011. Characterization and applications of as-grown Fe<sub>2</sub>O<sub>3</sub> nanoparticles prepared by hydrothermal method. *Journal of Nano particle Research*, 13: 3789-3799.
- Rajesh, K., Jai, S., Tiwari, R.S and Srivastava, O.N. 2012. Synthesis, characterization and optical properties of graphene sheets-ZnO multipod nanocomposites. *Journal of Alloys and Compounds*, 526: 129-134.
- Rusling, J.F. and Zhang, Z. 2003. Designing functional bimolecular films on electrodes. *Bimolecular Films*, 111: 1-64.
- Low, S.S., Tan, M.T.T., Loh, H.-S., Khiew P.S and Chiu, W.S. 2016. Facile hydrothermal growth. *Analytical chemistry*, 342-346.
- Sakaguchi, T., Morioka, Y., Yamasaki, M., Iwanaga, J., Beppu, K., Maeda, H., Morita, Y. and Tamiya, E. 2007. Rapid and onsite BOD sensing system using lumino bacterial immobilize chip. *Biosensor and Bioelectron*, 22(7): 1345-1350.
- Scholz, F. (Ed.). 2005. Electro analytical Methods Guide to Experiments and applications. *springer*, 50-56.
- Sensoy, R. T. Rosen, C. T. Ho and Karwe, M. V. 2006. Food Chemistry. *Journal of Biomaterials and Nanobiotechnology*, 4 : 17-27.
- Sharma, G.A., Kumar, D., Pathania and Sillanpa, M. 2016. Polyacrylamide@Zr(IV) vanadophosphenanocomposite: ion exchange properties, antibacterial activity, and photocatalytic behavior. *Journal of Indian Engineering Chemistry*, 33: 201-208.

- Silva, T.R., Westphal, E., Gallardo, H. and Vieira, I.C. 2014. Euro protective effect of catalpol against induced oxidative stress in mesencephalic neurons. *European Journal of Pharmacology*, 568:142-148.
- Srivastava, S., Kumar, S., Singh, V.N., Singh, M. and Vijay, Y.K. 2011. Synthesis and characterization of TiO<sub>2</sub> doped polyaniline composites for hydrogen gas sensing. *International Journal of Hydrogen Energy*, 36(10): 6343–6355.
- Stoller, M.D., Zhu, J. and Ruoff, R.S. 2008. Graphene-based ultracapacitors. *Nano Letters*, 8: 3498–502.
- Valls, S., Millán, M., Martí, P., Borràs, E. and Arola, L. 2009. Spectroscopic determination of phenol. *Journal of Chromatograph*, 216: 7143-7149.
- Wang, S.C., Zhang, Z., He, L.C. and Li, H. 2010. Non-aqueous capillary electrophoresis for separation and simultaneous determination of magnoflorine, taspine, and caulophine in *Caulophyllum robustum* collected in different seasons. *Analytical Letters*, 43: 1534–1542.
- Wu, J.X., Shen, L., Jiang, K., Wang and Chen, K. 2010. Capillary electrophoresis for phenol determination. *Applied Surface Science*, 256: 2826–2830.
- Yan-Ling, Yang, B., Unnikrishnan, S. and Ming, C. 2011. Amperometric determination of 4-nitrophenol at multi-walled carbon nanotube-Poly(Diphenylamine) composite modified glassy carbon electrode. *International journal of Electrochemical Science*, 6: 3902 – 3912.
- Yang, S., Feng, X., Ivanovici, S. and Mullen, K. 2010. Fabrication of graphene-encapsulated oxide nano particles: Towards high-performance anode materials for lithium storage. *Angew Chem Internatinal Education*, 49: 8408-8411.
- Yang, Y., Unnikrishnan, B. and Chen, S. 2011. Amperometric determination of 4-nitrophenol at multi-walled carbon nanotube-poly (diphenylamine) composite modified glassy carbon electrode. *Journal of Electrochemical Science*, 6: 3902-3912.
- Yao, L.H., Jiang, Y.M. and Shi, J. 2004. Flavonoids in food and their health benefits. *Plant Foods Human Nutrient*, 59(3): 113-122.

- Yin, H., Zhou, Y., Ai, S., Cui, L. and Zhu, L. 2010. Electrochemical determination of 2-nitrophenol in water samples using Mg-Al-SDS hydrotalcite-like clay modified glassy carbon electrode. *Electro analysis*, 22 (10): 1136–1142.
- Yin, Yunlei, Zhou, Shiyun, Ai, Xianggang, Liu, Lusheng, Zhu, Linan and Microchim. 2010. Electrochemical oxidative determination of 4 nitrophenol based on a glassy carbon electrode modified with a hydroxyl apatite nanopowder. *Actuator*, 169:87–92.
- Zhang, K., Lu, L., Wen, Y., Xu, J., Duan, X., Zhang, L., Hu, D and Nie, T. 2013. Facile nanohybrid and its application in electrochemical sensing of azithromycin. *Analytical chemistry*, 66.
- Zhang, T.T., Lang, Q.L., Yang, D.P., Li, L. and Zeng, L.X. 2013. Simultaneous voltammetric determination of nitrophenol isomers at ordered mesoporous carbon modified electrode. *Electrochemical Actuator*, 106: 127-130.

## **7.APPENDICES**

## 7.1. Appendix Tables

Appendix Table.1 Summary of electrochemical parameters for GCE evaluated from the CV of  $K_3Fe(CN)_6$  at different scan rates

Scan rate(mV/s)	Epa(mV)	Epc(mV)	Ipa(mA)	Ipc(mA)	Ipa/Ipc	$\Delta E$
10	188	165	0.045	0.064	0.7	23
30	230	160	0.057	0.079	0.72	70
50	238	148	0.063	0.089	0.76	90
100	240	146	0.0767	0.099	0.78	94

Appendix Table 2. Summary of electrochemical parameters for the different nanoparticles evaluated for the CV of FCN at scan rate of 50 mV/s

Nanocomposites	Epa(mV)	Epc(mV)	Ipa(mA)	Ipc(mA)	Ipa/Ipc	$\Delta E$
GCE	235	160	0.055	0.079	0.69	75
EGS/GCE	234	165	0.076	0.089	0.85	69
ZnO/GCE	195	230	0.085	0.099	0.86	35
EGS/ZnO/GCE	264	212	0.098	0.105	0.93	55

Appendix Table 3. Summary of electrochemical parameters for the different nanoparticles evaluated for the CV of 0.1M PBS at scan rate of 50 mV/s

Nanocomposites	E <sub>pa</sub> (mV)	E <sub>pc</sub> (mV)	I <sub>pa</sub> (mA)	I <sub>pc</sub> (mA)	I <sub>pa</sub> /I <sub>pc</sub>	ΔE
GCE	21	152	0.006	0.004	1.5	131
EGS/GCE	31	162	0.0064	0.006	1.06	131
ZnO/GCE	32	165	0.0095	0.0085	1.2	133
EGS/ZnO/GCE	36	167	0.011	0.01	1.1	131